Eur. Phys. J. A **1**, 171–186 (1998)

THE EUROPEAN PHYSICAL JOURNAL A

Thermodynamic properties of the $SU(2)_f$ chiral quark–loop soliton

M. Schleif, R. Wünsch[1]

Institut für Kern- und Hadronenphysik, Forschungszentrum Rossendorf e.V., Postfach 51 01 19, D-01314 Dresden, Germany

Received: 26 September 1997
Communicated by W. Weise

Abstract. We consider a chiral one-loop hedgehog soliton of the bosonized $SU(2)_f$ Nambu & Jona-Lasinio model which is embedded in a hot medium of constituent quarks. Energy and radius of the soliton are determined in self-consistent mean-field approximation. Quasi-classical corrections to the soliton energy are derived by means of the pushing and cranking approaches. The corresponding inertial parameters are evaluated. It is shown that the inertial mass is equivalent to the total internal energy of the soliton. Corrected nucleon and Δ isobar masses are calculated in dependence on temperature and density of the medium. As a result of the self-consistently determined internal structure of the soliton the scaling between constituent quark mass, soliton mass and radius is noticeably disturbed.

PACS. 12.39.Fe Chiral Lagrangians – 12.38.Lg Other nonperturbative calculations – 12.40.Yx Hadron mass models and calculations – 24.85.+p Quarks, gluons, and QCD in nuclei and nuclear processes

1 Introduction

Chiral soliton models have proven to be a fruitful approach to the description of nucleon structure. Starting from the Nambu & Jona-Lasinio (NJL) lagrangian [1] and applying a well defined scheme of approximations one was able to obtain stationary and localized field configurations denoted as non-topological chiral one-loop NJL solitons. They can be used to model nucleons, Δ isobars and strange baryons on the basis of interacting quarks (for review see [2,3]).

The NJL lagrangian incorporates chiral symmetry and its spontaneous breakdown [4]. It has been used to study the restoration of chiral symmetry in a hot and dense nuclear medium modeled by a gas of constituent quarks (for review see [5]). The decrease of the constituent quark mass at higher temperature and/or density of the medium describes the phase transition from the chiral condensate to the chirally symmetric phase. The calculated effects are in satisfactory agreement with the predictions of lattice calculations and of the chiral perturbation theory as well.

It is an attractive idea to combine both features of the NJL lagrangian and to study the behavior of a soliton embedded in a hot gas of constituent quarks with a dynamically generated mass. Such a model incorporates the restoration of chiral symmetry and the possible dissolution of the soliton, which simulates the deconfinement transition of hadronic matter. In contrast to many other approaches studying medium modifications the non-topological soliton model equips the baryon with an internal structure which may be modified by the medium.

Using this approach as a model for baryons in hot hadronic matter one should be aware of its approximative character which is even not free of inconsistencies. Below the critical values of temperature and density, the quark gas is not the ground state of strongly interacting matter, neither in nature nor within the model. If the soliton is stable the medium itself consists of solitons. This goes beyond the mean-field approach. The effect we can study within a mean-field picture is the scale change connected with the reduction of the constituent quark mass at increasing values of temperature and density and its effect on the self-consistent mean-field. Such an approach rests on the assumption that the dominating effect of the medium consists in the reduction of the constituent quark mass while its local variation is of minor importance. The free motion of the quarks representing the medium as a quark gas is an obvious shortcoming of the approach and may overestimate the influence of the medium on the soliton. There are attempts [6,7] to replace the quark degrees of freedom in a part of the effective action by nucleonic ones without introducing new parameters. The results are not very encouraging since chiral symmetry is restored already at normal nuclear density in this approach [6]. For a more detailed discussion see [8].

The soliton which we investigate is in most respects identical with the soliton described in [2,7,9]. The differences concern the particular treatment of the valence

Correspondence to: wuensch@fz-rossendorf.de

[1] Supported by the Bundesministerium für Bildung, Wissenschaft, Forschung und Technologie under contract No. 06 DR 666 I

quark level and the use of the chemical potential for adjusting the baryon number of the soliton.

Due to mean-field approximation and hedgehog ansatz the soliton has defects already known from the soliton in vacuum: it violates translational and (iso-)rotational invariance. Therefore it is affected by center-of-mass motion and represents a mixture of nucleon and Δ isobar instead of a particle with definite spin and isospin. The violated translational and rotational symmetries can approximately be restored. The quasi-classical pushing and cranking approaches [10] constitute a feasible way to exclude spurious contributions to the energy and to equip the soliton with the correct values of spin and isospin. The size of pushing and cranking corrections is controlled by inertial parameters. While we relate the inertial soliton mass to its total mean-field energy the (iso-)rotational moment of inertia is calculated numerically. The relation between inertial mass and internal energy, which is derived in this paper, is an extension of the corresponding relation for a soliton in vacuum [11].

In Sect. 2, we shortly outline the basic ideas defining the NJL soliton in a medium of constituent quarks at finite temperature and density and review the main formulae. We determine that region of density and temperature where a stable soliton exists. The baryon number of the soliton and its spatial distribution is considered in Sect. 3. Here we critically discuss the method to fix the baryon number to one, which was applied in [7]. The numerically determined soliton energies and radii are given and discussed in Sect. 4. In Sect. 5, we determine quasi-classical corrections to the soliton energy. We consider the soliton in a boosted and rotating frame and calculate the corresponding inertial parameters and energies. The corrected nucleon energies are given and discussed in Sect. 6. Conclusion are drawn in Sect. 7. An appendix completes the calculations in Sects. 2, 3 and 5.

2 NJL soliton in a heat bath

We consider an ensemble of up and down quarks with $N_c = 3$ colors and an average current mass $m = (m_u + m_d)/2$ at temperature T and chemical potential $\mu = \mu_u = \mu_d$. The latter will be related to temperature T and density ρ_0 of the medium embedding the soliton. The quarks interact via a four-quark contact interaction, which consists of a chirally symmetric combination of a scalar-isoscalar and a pseudoscalar-isovector term, with the coupling strength $G/2$ introduced by Nambu & Jona-Lasinio [1]. The soliton is defined by an *effective action* whose derivation from the $SU(2)_f$ NJL Lagrangian incorporates the following steps (for a review see [2,3]):

1. Introduction of auxiliary meson fields σ and $\boldsymbol{\pi}$ by means of a Hubbard-Stratonovich transformation [12,13] in the generating functional using the imaginary-time formalism.
2. Derivation of an effective meson action $\mathcal{A}_{\rm eff}[\sigma, \boldsymbol{\pi}]$ by applying the stationary phase approximation on the meson fields (no meson loops, σ and $\boldsymbol{\pi}$ as classical mean fields). The effective action obtained in this way consists of a purely *mesonic part* $\mathcal{A}^{\rm m}$ and of a *fermionic part* $\mathcal{A}^{\rm q}$. The latter describes the contributions of the various quark levels to the effective action (quark determinant).
3. Restriction of the meson fields to static and spherically symmetric hedgehog configurations $\big(\sigma(\boldsymbol{r},\tau) = \sigma(r)$, $\boldsymbol{\pi}(\boldsymbol{r},\tau) = \pi(r)\,\hat{\boldsymbol{r}}\big)$. In our numerical calculations, the meson fields will additionally be restricted to the chiral circle $\big(\sigma^2(r)+\pi^2(r) = \sigma_0^2 = \text{const}\big)$. Otherwise, a stable soliton does not exist [14,15].
4. Splitting the quark part of the effective action into a contribution $\mathcal{A}^{\rm q,sea}$ (*sea contribution*) which results from a completely occupied Dirac sea and a residual contribution $\mathcal{A}^{\rm q,med}(T,\mu)$ (*medium contribution*) which describes the occupation of the quark levels according to temperature and chemical potential (quarks in levels with positive energy and holes at negative energy). The sea contribution diverges and is regulated by means of Schwinger's proper-time regularization scheme [16]. The corresponding cut-off Λ is not considered as a free parameter but is related to the experimental values of the pion mass and of the weak pion-decay constant in vacuum [2,17,18].
5. Interaction strength G and cut-off parameter Λ are determined in the vacuum and assumed to be independent of T and μ. This assumption ensures the exact scaling between pion decay constant and constituent quark mass.
6. The soliton itself is defined as a localized deviation of the fields from their asymptotic values σ_0 and $\pi_0 = 0$ which describe the homogeneous medium. Solitonic expectation values are defined by the difference between the values obtained for solitonic and homogeneous field configurations.

The *relative effective action* of the soliton is obtained by subtracting the effective action $\mathcal{A}_{\rm eff}[\sigma_0, 0]$ of the homogeneous configuration from the effective action of the solitonic field

$$\begin{aligned}\mathcal{A}_{\rm eff}[\sigma,\pi;\sigma_0] &\equiv \mathcal{A}_{\rm eff}[\sigma,\pi] - \mathcal{A}_{\rm eff}[\sigma_0,0] \\ &= \mathcal{A}^{\rm m}[\sigma,\pi;\sigma_0] + \mathcal{A}^{\rm q}[\sigma,\pi;\sigma_0]\,.\end{aligned} \tag{1}$$

It consists of a purely mesonic part

$$\begin{aligned}\mathcal{A}^{\rm m}[\sigma,\pi;\sigma_0] = \frac{1}{2G}\frac{1}{T}\int \mathrm{d}^3\boldsymbol{r}\,\left[\sigma^2(\boldsymbol{r}) + \pi^2(\boldsymbol{r}) - \sigma_0^2\right] \\ + \frac{m}{G}\frac{1}{T}\int \mathrm{d}^3\boldsymbol{r}\,\left[\sigma_0 - \sigma(r)\right]\end{aligned} \tag{2}$$

and of the quark determinant which can be written

$$\begin{aligned}\mathcal{A}^{\rm q}[\sigma,\pi;\sigma_0](T,\mu) &= -N_c \mathrm{Tr}\ln\frac{D(\mu)}{D_0(\mu)} \\ &= \mathcal{A}^{\rm q,sea}[\sigma,\pi;\sigma_0] + \mathcal{A}^{\rm q,med}[\sigma,\pi;\sigma_0](T,\mu)\end{aligned} \tag{3}$$

with

$$\mathcal{A}^{\rm q,sea}[\sigma,\pi;\sigma_0] = -\frac{1}{T}N_c \lim_{T\to 0} T\mathrm{Tr}\ln\frac{D(0)}{D_0(0)} \tag{4}$$

and

$$\mathcal{A}^{\mathrm{q,med}}[\sigma,\pi;\sigma_0](T,\mu) = \mathcal{A}^{\mathrm{q}} - \mathcal{A}^{\mathrm{q,sea}} \tag{5}$$
$$= -N_\mathrm{c}\mathrm{Tr}\ln\frac{D(\mu)}{D_0(\mu)} + \frac{1}{T}N_\mathrm{c}\lim_{T\to 0} T\mathrm{Tr}\ln\frac{D(0)}{D_0(0)}$$

with the trace Tr defined in appendix A. While the medium contribution (5) is finite and vanishes in the limit $(T,\mu)\to 0$ the sea contribution (4) diverges and does not explicitly depend on the thermodynamical variables. The latter is regularized by replacing the operator trace Tr (A.2) by a regularized trace Tr_Λ (A.3). The single-particle operators

$$D(\mu) = \partial_\tau + h - \mu\,, \tag{6}$$
$$D_0(\mu) = \partial_\tau + h_0 - \mu \tag{7}$$

consist of the derivative ∂_τ with respect to the euclidean time coordinate τ, the quark hamiltonians

$$h \;\equiv\; h(\sigma,\pi) \;=\; \boldsymbol{\alpha}\cdot\boldsymbol{p} + \beta\left[\sigma(r) + \mathrm{i}\gamma_5\boldsymbol{\tau}\cdot\hat{\boldsymbol{r}}\,\pi(r)\right]\,, \tag{8}$$
$$h_0 \equiv\; h(\sigma_0,0) =\; \boldsymbol{\alpha}\cdot\boldsymbol{p} + \beta\,\sigma_0\,, \tag{9}$$

and the chemical potential μ. The Dirac matrices are denoted by $\beta\equiv\gamma^0$, $\boldsymbol{\gamma}\equiv(\gamma^1,\gamma^2,\gamma^3)$, $\gamma_5\equiv\mathrm{i}\gamma^0\gamma^1\gamma^2\gamma^3$, $\boldsymbol{\alpha}\equiv\beta\boldsymbol{\gamma}$, and $\boldsymbol{\tau}$ is the vector of Pauli matrices. Spatial coordinates are denoted by $\boldsymbol{r}$ and have the components r^i, the absolute value $r\equiv|\boldsymbol{r}|$ and unit vector $\hat{\boldsymbol{r}}\equiv\boldsymbol{r}/r$.

The crucial quantity for the description of a grand canonical ensemble of quarks is the thermodynamical (grand canonical) potential given by

$$\Omega(T,\mu) = T\mathcal{A}_\mathrm{eff} = \Omega^\mathrm{m} + \Omega^\mathrm{q}(T,\mu) \tag{10}$$

with

$$\Omega^{\mathrm{m,q}} = T\mathcal{A}^{\mathrm{m,q}}\,. \tag{11}$$

On the analogy of the effective action we split the quark part of the canonical potential into a sea and a medium contribution

$$\Omega^\mathrm{q}(T,\mu) = -N_\mathrm{c}T\mathrm{Tr}_\Lambda\ln\frac{D(\mu)}{D_0(\mu)} = \Omega^{\mathrm{q,sea}}_\Lambda + \Omega^{\mathrm{q,med}}(T,\mu) \tag{12}$$

where Tr_Λ means regularization of only the sea contribution. For time-independent meson fields the determinants of the inverse propagators (6, 7) are real and the regularized sea contribution can be written

$$\Omega^{\mathrm{q,sea}}_\Lambda = -\frac{N_\mathrm{c}}{2}\lim_{T\to 0} T\mathrm{Tr}_\Lambda\ln\frac{D^\dagger(0)\,D(0)}{D_0^\dagger(0)\,D_0(0)}\,. \tag{13}$$

In the proper-time scheme, we get by means of (A.3)

$$\Omega^{\mathrm{q,sea}}_\Lambda = \frac{N_\mathrm{c}}{2}\int\limits_{1/\Lambda^2}^{\infty}\frac{\mathrm{d}s}{s}\int\limits_{-\infty}^{\infty}\frac{\mathrm{d}\omega}{2\pi} \tag{14}$$
$$\times\sum_\alpha\left[\mathrm{e}^{-s(\omega^2+\varepsilon_\alpha^2)} - \mathrm{e}^{-s(\omega^2+(\varepsilon^0_\alpha)^2)}\right]$$
$$= -\frac{N_\mathrm{c}}{2}\sum_\alpha\left[R_\mathrm{E}(\varepsilon_\alpha,\Lambda)\,|\varepsilon_\alpha| - R_\mathrm{E}(\varepsilon^0_\alpha,\Lambda)\,|\varepsilon^0_\alpha|\right]$$

where ε_α (ε^0_α) are the eigenvalues of the quark hamiltonians h (h_0) defined in (8, 9), and R_E is the regularization function

$$R_\mathrm{E}(\varepsilon,\Lambda) = -\frac{1}{\sqrt{4\pi}}\,\Gamma\left(-\frac{1}{2},\frac{\varepsilon^2}{\Lambda^2}\right) \tag{15}$$

with the incomplete Gammafunction $\Gamma(x,a)$. Notice that the degeneration with respect to the color degree of freedom is explicitly taken into account by the factor N_c and included neither in the trace Tr nor in the sum over α.

The medium contribution to the quark part of the canonical potential (12) is finite and will not be regularized. One gets by means of (A.1–A.5)

$$\Omega^{\mathrm{q,med}}(T,\mu) = -N_\mathrm{c}T\mathrm{Tr}\ln\frac{D(\mu)}{D_0(\mu)} + N_\mathrm{c}\lim_{T\to 0} T\mathrm{Tr}\ln\frac{D(0)}{D_0(0)}$$
$$= -N_\mathrm{c}\mu\,B^\mathrm{sea} - N_\mathrm{c}T\sum_\alpha\ln\frac{1+\mathrm{e}^{-\mathrm{sign}(\varepsilon_\alpha)\,(\varepsilon_\alpha-\mu)/T}}{1+\mathrm{e}^{-\mathrm{sign}(\varepsilon^0_\alpha)\,(\varepsilon^0_\alpha-\mu)/T}}\,. \tag{16}$$

The medium contribution depends on the thermal occupation probability of the various quark levels which are controlled by temperature and chemical potential. The quantity

$$B^\mathrm{sea} = -\sum_\alpha\frac{\mathrm{sign}(\varepsilon_\alpha)}{2} \tag{17}$$

describes the baryon number of the Dirac sea for the solitonic field. Usually the number of quark levels with positive and negative energy are equal and B^sea vanishes. It differs from zero only if the meson field is strong enough to pull down one or more quark levels from the positive continuum into the negative energy region. This happens at rather large interaction strength G corresponding to vacuum constituent quark masses $M \gtrsim 700\,\mathrm{MeV}$, and we shall not consider this case here.

Customarily one treats the contribution of the valence level (α=val) to the medium part (16) separately, ascribes occupation number one to this level ($\tilde{n}_{\varepsilon_\mathrm{val}}=1$) and leaves it empty in the homogeneous medium ($\tilde{n}_{\varepsilon^0_\mathrm{val}}=0$) [9]. This is the simplest way to realize a soliton with baryon number one in a cold medium. However, the hole in the homogeneous configuration has serious consequences for the size of the iso-rotational moment of inertia which will be studied in Sect. 5.2.

The rule to regularize only the sea contribution to the quark determinant should be considered as an ingredient of the model. It does not reproduce the correct limit $T\to\infty$ but dealing with a low-energy model we need not consider this case. In our case, the regularization procedure would have a negligible effect on the medium contribution since the cut-off is larger than chemical potential and temperature ($\Lambda > \mu + T$). Moreover it simplifies the model considerably since it decouples the regularization procedure from temperature and density dependence.

The classical meson fields σ and π minimize the grand canonical potential (10)

$$\frac{\delta\Omega(T,\mu)}{\delta\sigma(\boldsymbol{r})} = 0 \qquad \text{and} \qquad \frac{\delta\Omega(T,\mu)}{\delta\pi(\boldsymbol{r})} = 0 \tag{18}$$

leading to the equations of motion

$$\sigma(\boldsymbol{r}) = m - G\left\langle\!\left\langle \bar{q}(\boldsymbol{r})\, q(\boldsymbol{r})\right\rangle\!\right\rangle, \tag{19}$$

$$\pi(\boldsymbol{r}) = -G\left\langle\!\left\langle \bar{q}(\boldsymbol{r})\, \mathrm{i}\gamma_5 \boldsymbol{\tau}\cdot\hat{\boldsymbol{r}}\, q(\boldsymbol{r})\right\rangle\!\right\rangle . \tag{20}$$

In general, the equations of motion can only numerically be solved since the thermal expectation values $\langle\langle \ldots \rangle\rangle$ on the right sides depend functionally on the fields on the left sides. Expectation values of currents such as in (19, 20) will be evaluated in Sect. 3. A particular solution of the equations of motion is given by homogeneous fields $\sigma(\boldsymbol{r}) \equiv \sigma_0$ and $\pi(\boldsymbol{r}) \equiv 0$ where σ_0 has to fulfill the gap equation which follows from (19). A constant sigma field acts as a mass on the quarks and $\sigma_0(T,\mu)$ is identified with the constituent quark mass M^*. Its value M at $T = \mu = 0$ is the only free parameter of the model, which can vary within reasonable limits (see e. g. [2]). It determines the strength G of the quark-quark interaction in the initial NJL lagrangian. Keeping G fixed the constituent mass M^* for finite values of temperature and density is uniquely determined by the gap equation. We chose $M = 420\,\mathrm{MeV}$ in the numerical calculations. This value reproduces the experimental Δ-nucleon splitting.

A solution of the equation of motion is called a self-consistent field configuration since one considers not only the explicit dependence of Ω (10) on the meson fields via Ω^{m} but also the dependence via energy spectrum $\{\varepsilon_\alpha\}$ of the quarks which enters the parts $\Omega_\Lambda^{\mathrm{q,sea}}$ (13) and $\Omega^{\mathrm{q,med}}$ (16). Restricting the meson fields to the chiral circle σ and π fields are not independent of each other and equations (19, 20) can be replaced by a single one e. g. for the chiral angle $\theta(r)$ (see e. g. [19]). We consider hedgehog fields with winding number one characterized by the boundary conditions $\theta(r=0) = -\pi$ and $\theta(r\to\infty) = 0$.

The lack of confinement in the NJL model forces us to exclude the valence level from the thermal equilibrium and to keep its occupation probability fixed to one independently of temperature and chemical potential as proposed in [7]. The valence quarks play a crucial role for the existence of self-consistent solitonic field configurations. Only the valence quarks yield a spatially restricted negative contribution to the expectation value on the right side of the equation of motion (19) leading to a well in the σ field. The soliton is stable if the well is deep enough to bind the valence quarks. If one occupies the valence level according to the thermal occupation probability, which is smaller than one, the resulting well binds the quarks weaker, and – starting from a critical temperature – a homogeneous field with free quarks is the only self-consistent solution of the equations of motion. This happens already at temperatures around 100 MeV far away from the expected transition point to the quark plasma. Keeping the occupation number of the valence level fixed the plasma transition takes place at reasonable temperatures around 180 MeV. This transition does not coincide with the restoration of chiral symmetry indicated by the reduction of the constituent quark mass M^* to the value of the current mass m. The constituent mass is only reduced to half of its vacuum value when the soliton dissolves.

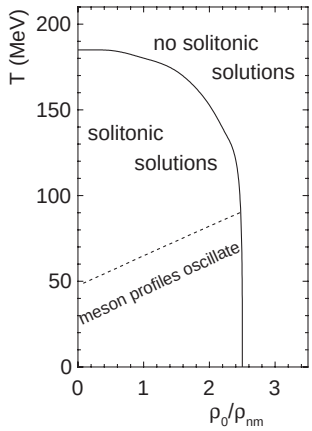

Fig. 1. Region in the $T-\rho_0$ plane where solitonic field configurations have been found for $M = 420\,\mathrm{MeV}$. The density ρ_0 is given in units of the normal nuclear density $\rho_{\mathrm{nm}} = 0.16\,\mathrm{fm}^{-3}$. In the *region below the broken line* the self-consistent meson fields exhibit pronounced oscillations outside the soliton in the course of the iterative solution of the equation of motion

Figure 1 outlines that region in the $T-\rho_0$ plane where we have obtained stable, self-consistent solitonic field configurations. The medium density ρ_0 is related to T and μ via (45). The region with temperatures $T \lesssim 75\,\mathrm{MeV}$ (below the broken line in Fig. 1) has to be considered with some caution since we performed our numerical calculations within a discrete basis [20] by introducing a box with radius D. Below 75 MeV, the meson fields start to oscillate during the iteration and the final results are very sensitive to the box radius. The finite box radius produces an artificial spacing and shift of the quark levels which are proportional to $1/D$. Shift and spacing are important in a transition region around the Fermi energy where the occupation probability varies rapidly. The width of the transition region is proportional to the temperature. In the course of the iteration the levels in the sensitive transition region around the Fermi level change rapidly their contribution to the mean field with a significant effect on its shape. The calculation is stable if a larger number of levels lies within the transition region, i. e. if the level spacing is sufficiently smaller than the transition region. At low temperatures the spacing has to be rather small and the basis for a reliable calculation must be large. In this way the capacity of the computer determines a lower temperature limit for a reliable calculation. We used a box with radius $D = 18/M^*$ which restricts ourselves to temperatures above the broken line in Fig. 1. In contrast to finite medium density a calculation at vanishing density is not affected by the level spacing. In this case, the Fermi energy lies in the middle of the energy gap between $\pm M^*$ and there are no quark levels in the sensitive region.

At temperatures and densities above the solid line in Fig. 1 a solitonic solution of the equations of motion (19, 20) has not been found. Here the self-consistent meson field is too shallow to bind quarks.

Knowing the grand canonical potential Ω the free energy F of the soliton can be obtained by means of a Leg-

endre transformation replacing the independent variable μ by the baryon number $B = -\partial\Omega/(N_\mathrm{c}\,\partial\mu)$. The internal energy is obtained by an additional Legendre transformation from the dependence on temperature to entropy $S = -\partial\Omega/\partial T$. Analogously to the effective action we split internal and free energy into mesonic, regularized quark-sea and quark-medium contributions and subtract the corresponding energies of the homogeneous medium

$$E = E^\mathrm{m} + E_\Lambda^\mathrm{q,sea} + E^\mathrm{q,med}\,, \tag{21}$$

$$F = F^\mathrm{m} + F_\Lambda^\mathrm{q,sea} + F^\mathrm{q,med}\,. \tag{22}$$

Since mesonic and sea contributions to the grand canonical potential are independent of T and μ we have

$$E^\mathrm{m} = F^\mathrm{m} = \Omega^\mathrm{m} \tag{23}$$

and

$$E_\Lambda^\mathrm{q,sea} = F_\Lambda^\mathrm{q,sea} = \Omega_\Lambda^\mathrm{q,sea}\,. \tag{24}$$

The medium contributions are given by

$$E^\mathrm{q,med} = \left[1 - T\frac{\partial}{\partial T} - \mu\frac{\partial}{\partial\mu}\right]\Omega^\mathrm{q,med}(T,\mu) \tag{25}$$

$$= N_\mathrm{c}\sum_\alpha\left[\tilde{n}_{\varepsilon_\alpha}(T,\mu)\,\varepsilon_\alpha - \tilde{n}_{\varepsilon_\alpha^0}(T,\mu)\,\varepsilon_\alpha^0\right]$$

and

$$F^\mathrm{q,med} = \left[1 - \mu\frac{\partial}{\partial\mu}\right]\Omega^\mathrm{q,med}(T,\mu) \tag{26}$$

$$= N_\mathrm{c}\sum_\alpha\left[T\ln\Big(1-\mathrm{sign}(\varepsilon_\alpha)\,\tilde{n}_{\varepsilon_\alpha}(T,\mu)\Big) + \mu\,\tilde{n}_{\varepsilon_\alpha}(T,\mu)\right]$$
$$-N_\mathrm{c}\sum_\alpha\left[T\ln\Big(1-\mathrm{sign}(\varepsilon_\alpha^0)\,\tilde{n}_{\varepsilon_\alpha^0}(T,\mu)\Big) + \mu\,\tilde{n}_{\varepsilon_\alpha^0}(T,\mu)\right]$$

where we have introduced the modified occupation number

$$\tilde{n}_{\varepsilon_\alpha}(T,\mu) = \frac{1}{1+\mathrm{e}^{(\varepsilon_\alpha-\mu)/T}} - \Theta\Big(-\varepsilon_\alpha\Big) \tag{27}$$

$$= \frac{\mathrm{sign}(\varepsilon_\alpha)}{1+\mathrm{e}^{\mathrm{sign}(\varepsilon_\alpha)\,(\varepsilon_\alpha-\mu)/T}}$$

which describes the thermodynamical probability to find an occupied level at positive energy ε_α and a hole at negative energy, respectively. The latter is supplied with a minus sign. For the completely occupied Dirac sea without any additional quarks above it we have $\tilde{n}_{\varepsilon_\alpha}(0,0) = 0\ \forall\alpha$.

3 Baryon number, density and chemical potential

Now let us investigate the baryon number B of the self-consistently determined solitonic field and their spatial distribution $\rho(\boldsymbol{r})$. For that aim we consider thermal expectation values $\langle\!\langle O\rangle\!\rangle$ of one-body quark operators

$$O = \int \mathrm{d}^3\boldsymbol{r}\; q^\dagger(\boldsymbol{r})\,\mathcal{O}\,q(\boldsymbol{r}) \tag{28}$$

where $\mathcal{O}$ is a time-independent operator acting in the Dirac and/or flavor (isospin) space. The baryon number is obtained with $\mathcal{O}=1/N_\mathrm{c}$.

To calculate thermal expectation values of one-body quark operators (28) we define a generating function

$$\Omega_{(\Lambda)}^\mathrm{q}(T,\mu;\kappa) = -N_\mathrm{c}T\mathrm{Tr}_{(\Lambda)}\ln\frac{D(\mu;\kappa)}{D_0(\mu;\kappa)} \tag{29}$$
$$= \Omega_{(\Lambda)}^\mathrm{q,sea}(\kappa) + \Omega^\mathrm{q,med}(T,\mu;\kappa)$$

given by the canonical quark potential (12) with the inverse propagators $D_{(0)}(\mu)$ replaced by

$$D_{(0)}(\mu;\kappa) = D_{(0)}(\mu) - \kappa\mathcal{O} = \partial_\tau + h_{(0)} - \mu - \kappa\mathcal{O}\,. \tag{30}$$

Restricting the meson fields to their classical values the mesonic part of the grand canonical potential does not influence expectation values. We shall use both the unregularized version

$$\Omega^\mathrm{q,sea}(\kappa) = -N_\mathrm{c}\lim_{T\to0}T\mathrm{Tr}\ln\frac{D(0;\kappa)}{D_0(0;\kappa)} \tag{31}$$

and the regularized version $\Omega_\Lambda^\mathrm{q,sea}(\kappa)$ of the sea contribution to (29) with Tr replaced by Tr_Λ. The medium contribution to the extended canonical potential (29) is given by

$$\Omega^\mathrm{q,med}(T,\mu;\kappa) \tag{32}$$
$$= -N_\mathrm{c}T\mathrm{Tr}\ln\frac{D(\mu;\kappa)}{D_0(\mu;\kappa)} + N_\mathrm{c}\lim_{T\to0}T\mathrm{Tr}\ln\frac{D(0;\kappa)}{D_0(0;\kappa)}\,.$$

Expectation values of an operator (28) can be expressed by

$$\langle\!\langle O\rangle\!\rangle = -\left.\frac{\mathrm{d}\Omega_{(\Lambda)}^\mathrm{q}(T,\mu;\kappa)}{\mathrm{d}\kappa}\right|_{\kappa=0} = \langle O\rangle_{(\Lambda)}^\mathrm{sea} + \langle\!\langle O\rangle\!\rangle^\mathrm{med} \tag{33}$$

with the unregularized sea contribution

$$\langle O\rangle^\mathrm{sea} \equiv -\left.\frac{\mathrm{d}\Omega^\mathrm{q,sea}(\kappa)}{\mathrm{d}\kappa}\right|_{\kappa=0} \tag{34}$$
$$= -N_\mathrm{c}\lim_{T\to0}T\mathrm{Tr}\Big[\Big(D(0)^{-1} - D_0(0)^{-1}\Big)\,\mathcal{O}\Big]$$
$$= -\frac{N_\mathrm{c}}{2}\sum_\alpha\Big[\mathrm{sign}(\varepsilon_\alpha)\,O_\alpha - \mathrm{sign}(\varepsilon_\alpha^0)\,O_\alpha^0\Big]$$

and the medium contribution

$$\langle\!\langle O\rangle\!\rangle^\mathrm{med} \equiv -\left.\frac{\mathrm{d}\Omega^\mathrm{q,med}(T,\mu;\kappa)}{\mathrm{d}\kappa}\right|_{\kappa=0} \tag{35}$$
$$= N_\mathrm{c}\sum_\alpha\Big[\tilde{n}_{\varepsilon_\alpha}(T,\mu)\,O_\alpha - \tilde{n}_{\varepsilon_\alpha^0}(T,\mu)\,O_\alpha^0\Big]$$

with the modified occupation numbers $\tilde{n}_{\varepsilon_\alpha^{(0)}}(T,\mu)$ (27) and the matrix elements

$$O_\alpha^{(0)} = \left\langle \alpha^{(0)} \left| \mathcal{O} \right| \alpha^{(0)} \right\rangle = \int \mathrm{d}^3\boldsymbol{r}\, \Phi_\alpha^{(0)\,\dagger}(\boldsymbol{r})\, \mathcal{O}\, \Phi_\alpha^{(0)}(\boldsymbol{r}) \quad (36)$$

of the operator $\mathcal{O}$ with the normalized eigenfunctions $\Phi_\alpha^{(0)}(\boldsymbol{r})$ of the hamiltonian $h\,(h_0)$. Sea contributions such as expression (34) are defined as expectation values at zero temperature and we use the single brackets instead of the double ones which stand for a thermal expectation value. In fact, the sea contribution is not completely independent of T and μ but depends on them via the self-consistent mean fields σ and π. Using the regularized version of the sea contribution (31) we get the regularized expectation value

$$\langle O \rangle_\Lambda^{\mathrm{sea}} = -\frac{N_\mathrm{c}}{2} \sum_\alpha \left[R_\mathrm{m}(\varepsilon_\alpha, \Lambda)\, O_\alpha - R_\mathrm{m}(\varepsilon_\alpha^0, \Lambda)\, O_\alpha^0 \right]. \quad (37)$$

In the proper-time scheme, the regularization function is given by

$$R_\mathrm{m} = \frac{\mathrm{sign}(\varepsilon)}{\sqrt{\pi}}\, \Gamma\left(\frac{1}{2}, \frac{\varepsilon^2}{\Lambda^2}\right) = \mathrm{erf_c}\,(\varepsilon/\Lambda) \quad (38)$$

with the complementary error-function $\mathrm{erf_c}(x) = \frac{2x}{\sqrt{\pi}} \int_1^\infty \mathrm{d}t\, \mathrm{e}^{-t^2x^2}$. Inserting $\mathcal{O} = 1/N_\mathrm{c}$ one gets the solitonic baryon number

$$B = \left\langle\!\!\left\langle \frac{1}{N_\mathrm{c}} \int \mathrm{d}^3\boldsymbol{r}\, q^\dagger(\boldsymbol{r})\, q(\boldsymbol{r}) \right\rangle\!\!\right\rangle \quad (39)$$

$$= B^{\mathrm{sea}} + \sum_\alpha \left[\tilde{n}_{\varepsilon_\alpha}(T,\mu) - \tilde{n}_{\varepsilon_\alpha^0}(T,\mu) \right]$$

with the unregularized sea contribution introduced in (17). The same expression is obtained if one starts from the grand canonical potential (10) and uses the thermodynamical relation $B = -\partial\Omega/(N_\mathrm{c}\,\partial\mu)$ keeping in mind that the meson fields have to minimize the potential (18).

To investigate the properties of a soliton which is embedded in a medium with given density ρ_0 we have to establish a relation between T, ρ_0 and μ. This will be done below (45). Knowing T and μ one can determine the solitonic field by means of the equations of motion (19, 20). Its baryon number (39) varies with T and μ and is different from one in general. The usual method to get a state with definite baryon number by minimizing the free energy can not be applied since it changes the chemical potential which has already uniquely been determined by the medium density ρ_0. In [7], a chemical potential μ_s for the solitonic field configuration was introduced, which differs from the chemical potential μ of the homogeneous field, in order to fix the solitonic baryon number exactly to one. However, such a soliton is spatially unlimited since a finite fraction of the baryon number is uniformly spread over the whole space. To elucidate this statement we consider the baryon density which is defined as the expectation value of the current

$$O(\boldsymbol{r}) = q^\dagger(\boldsymbol{r})\, \mathcal{O}\, q(\boldsymbol{r})\,. \quad (40)$$

with $\mathcal{O} = 1/N_\mathrm{c}$. The expectation value of currents (40) with a time-independent operator $\mathcal{O}$ can be treated in a way similar to the expectation value of the operator (28). One defines a generating functional $\Omega^\mathrm{q}[\kappa](T,\mu)$ by formally the same expression (29) but with a space-dependent function $\kappa(\boldsymbol{r})$ instead of the parameter κ. The corresponding expectation values are obtained by (34–38) with the derivative $\mathrm{d}/\mathrm{d}\kappa$ replaced by the functional derivative $\delta/\delta\kappa(\boldsymbol{r})$ and the matrix elements

$$O_\alpha^{(0)}(\boldsymbol{r}) = \Phi_\alpha^{(0)\,\dagger}(\boldsymbol{r})\, \mathcal{O}\, \Phi_\alpha^{(0)}(\boldsymbol{r}) \quad (41)$$

instead of the matrix elements (36). The expectation values in the equations of motion (19, 20) are of the same type and can be obtained with $\mathcal{O} = \gamma^0$ and $\mathcal{O} = \mathrm{i}\gamma^0\gamma_5 \boldsymbol{\tau}\cdot\hat{\boldsymbol{r}}$, respectively. Applied to the baryon density we get

$$\rho(\boldsymbol{r}) = -T \int_0^{1/T} \mathrm{d}\tau \left\langle \boldsymbol{r}\tau \left| \,\mathrm{tr}\left[D(\mu)^{-1} - D_0(\mu)^{-1}\right] \right| \boldsymbol{r}\tau \right\rangle \quad (42)$$

$$= \rho^{\mathrm{sea}}(\boldsymbol{r}) + \rho^{\mathrm{med}}(\boldsymbol{r})$$

with

$$\rho^{\mathrm{sea}}(\boldsymbol{r}) = -\frac{1}{2} \sum_\alpha \Big[\mathrm{sign}(\varepsilon_\alpha)\, \Phi_\alpha^\dagger(\boldsymbol{r})\, \Phi_\alpha(\boldsymbol{r}) - \mathrm{sign}(\varepsilon_\alpha^0)\, \Phi_\alpha^{0\,\dagger}(\boldsymbol{r})\, \Phi_\alpha^0(\boldsymbol{r}) \Big], \quad (43)$$

$$\rho^{\mathrm{med}}(\boldsymbol{r}) = \sum_\alpha \Big[\tilde{n}_{\varepsilon_\alpha}(T,\mu)\, \Phi_\alpha^\dagger(\boldsymbol{r})\, \Phi_\alpha(\boldsymbol{r}) - \tilde{n}_{\varepsilon_\alpha^0}(T,\mu)\, \Phi_\alpha^{0\,\dagger}(\boldsymbol{r})\, \Phi_\alpha^0(\boldsymbol{r}) \Big]. \quad (44)$$

Integrating over the whole space we recover the total baryon number (39).

First let us consider the homogeneous medium characterized by the hamiltonian h_0 with a constant σ field $\sigma_0 = M^*$ and vanishing π field. The corresponding eigenfunctions are plane waves characterized by the momentum vector $\boldsymbol{k}$ and normalized to one particle in the volume $\mathcal{V}$. The sea contribution (43) vanishes, and the sum $\sum_\alpha$ in the medium contribution (44) has to be replaced by an integral $4\mathcal{V}\int \frac{\mathrm{d}^3\boldsymbol{k}}{(2\pi)^3}$ taking into account both signs of the energies $\pm\varepsilon_k$ with $\varepsilon_k = \sqrt{\boldsymbol{k}^2 + M^{*\,2}}$, and spin and isospin degeneration as well. One gets

$$\rho_0 = \frac{2}{\pi^2} \int_0^\infty \mathrm{d}k\, k^2 \left[\tilde{n}_{\varepsilon_k}(T,\mu) + \tilde{n}_{-\varepsilon_k}(T,\mu) \right] \quad (45)$$

$$= \frac{2}{\pi^2} \int_0^\infty \mathrm{d}k\, k^2 \left[\frac{1}{1+\mathrm{e}^{(\varepsilon_k - \mu)/T}} - \frac{1}{1+\mathrm{e}^{(\varepsilon_k + \mu)/T}} \right].$$

Equation (45) establishes a relation between medium density and chemical potential and is used to determine μ for a given medium density ρ_0 and temperature T. It is also used to test the accuracy of the numerical procedure and to determine the necessary size of the basis. For that aim

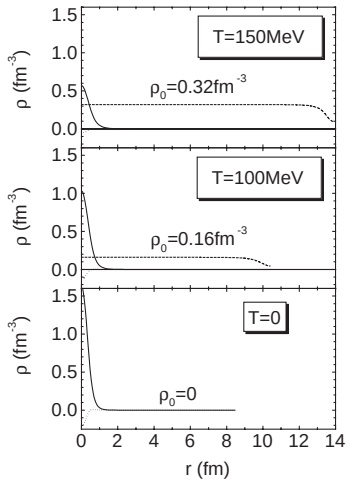

Fig. 2. Baryon density distribution of the soliton (*full lines*) normalized to baryon number $B = 4\pi\int \mathrm{d}r\, r^2\rho(r)$ as a function of the distance r from the center. The *broken lines* show the reproduction of the medium density by the discrete basis. The contributions of the Dirac sea are given by the *dotted lines*. The *right end of the curves* indicates the size of the box ($D = 18/M^*$), which is different in all three cases

we evaluate the baryon density for a homogeneous σ field by means of (44) within the discrete basis and check the agreement with the result (45) obtained in the momentum basis. We increase the basis until sufficient agreement is reached. The result is shown in Fig. 2 (dashed lines). Apart from a region close to the edge of the box, which is sufficiently far away from the soliton, the medium density is well reproduced by the discrete basis with a finite number of states.

The size of the various contributions to the solitonic baryon density (42) and their modification when changing the medium parameters from the vacuum to values close to the border of instability is illustrated in Fig. 2. The dominating contribution results from the valence part ($\alpha = \mathrm{val}$) of the medium contribution (44) giving rise to the bump around the center of the soliton. The residual terms in the medium contribution describe the polarization of the Fermi sea. Their contribution to the density is too small to be visible in Fig. 2. However, this contribution is located at larger distances than the valence contribution and has a remarkable influence on the soliton radius. Moreover it depends on temperature and density and contributes to the total baryon number. It is just this part of the total baryon number which is responsible for the deviation from one. The contribution (43) resulting from the polarization of the Dirac sea (dotted lines) modifies the density distribution but does not contribute to the baryon number (39). Figure 2 illustrates nicely the swelling of the soliton when increasing temperature and density. The mean-square radius of the soliton will systematically be studied in Sect. 4.

Now let us consider the consequences of introducing a chemical potential $\mu_\mathrm{s} = \mu + \delta\mu$ for the soliton which is different from the μ for the homogeneous background field. In this case (42) has to be replaced by

$$\rho(\boldsymbol{r}) = -T \int_0^{1/T} \mathrm{d}\tau \left\langle \boldsymbol{r}\tau \,\middle|\, \mathrm{tr}\big[D(\mu_\mathrm{s})^{-1} - D_0(\mu)^{-1}\big] \,\middle|\, \boldsymbol{r}\tau \right\rangle . \tag{46}$$

In the asymptotic region far away from the center of the soliton ($r \gg R$) we can replace the quark propagator $D(\mu_\mathrm{s})^{-1}$ by the propagator $D_0(\mu_\mathrm{s})^{-1}$ in the homogeneous field with the chemical potential for the soliton. This can be proven by expanding $D(\mu_\mathrm{s})^{-1}$ in (46) around $D_0(\mu_\mathrm{s})^{-1}$ (gradient expansion). As a result, the propagators differ only by terms which are proportional to the deviations of σ and π from their asymptotic values and by terms proportional to their derivatives which vanish in the asymptotic region. So we get

$$\begin{aligned}\rho(r \gg R) &= -T \int_0^{1/T} \mathrm{d}\tau \left\langle \boldsymbol{r}\tau \right| \mathrm{tr}\left[D_0(\mu_\mathrm{s})^{-1} - D_0(\mu)^{-1}\right] \left| \boldsymbol{r}\tau \right\rangle \\ &= \sum_\alpha \left[\tilde{n}_{\varepsilon_\alpha^0}(T,\mu_\mathrm{s}) - \tilde{n}_{\varepsilon_\alpha^0}(T,\mu)\right] \Phi_\alpha^{0\,\dagger}(\boldsymbol{r})\, \Phi_\alpha^0(\boldsymbol{r}) \end{aligned} \tag{47}$$

with the result that the soliton density vanishes at large distances from the center only if the chemical potentials μ and μ_s are equal. Introducing a different chemical potential μ_s one modifies the occupation probability for quarks in unbound states which contribute to observables at large distances. As a result, a finite fraction of the baryon number (and of other observables as well) is uniformly spread over the whole space. The root mean square (r.m.s.) radius $\bar{R}^*$ defined by

$$\bar{R}^* = \sqrt{\frac{\int \mathrm{d}^3\boldsymbol{r}\, r^2 \rho(\boldsymbol{r})}{\int \mathrm{d}^3\boldsymbol{r}\, \rho(\boldsymbol{r})}} \tag{48}$$

is infinitely large. The occurrence of unbound quark states below critical temperature and density is a consequence of the missing confinement in the NJL model. The situation is different for an isolated soliton at $T = 0$. Here one gets the soliton by adding 3 quarks onto the bound valence level which does not contribute to the density at large distances. As soon as $T > 0$ and/or $\varrho_0 > 0$ unbound quark levels are involved and the lack of confinement becomes evident.

The difference $\delta\mu$ between solitonic and medium chemical potential which is necessary to ensure $B = 1$ amounts to a few hundreds of keV and decreases as $1/D^3$ with increasing box radius D. The resulting solitonic density at large radii decreases correspondingly. It vanishes in the limit $D \to \infty$ and the effect might be considered as a box effect. Unfortunately that is not true. Independently of the box size a finite fraction of the baryon number is homogeneously spread outside the soliton, i. e. we have $\int_\mathcal{R}^\infty \mathrm{d}r\, r^2\rho(r) \neq 0$ outside any sphere with radius $\mathcal{R}$ around the soliton, and the mean-squared radius (48) diverges. In [7], the (small) deviation from the medium density outside the soliton was simply neglected, while it was taken into account when calculating the baryon number B. Similar

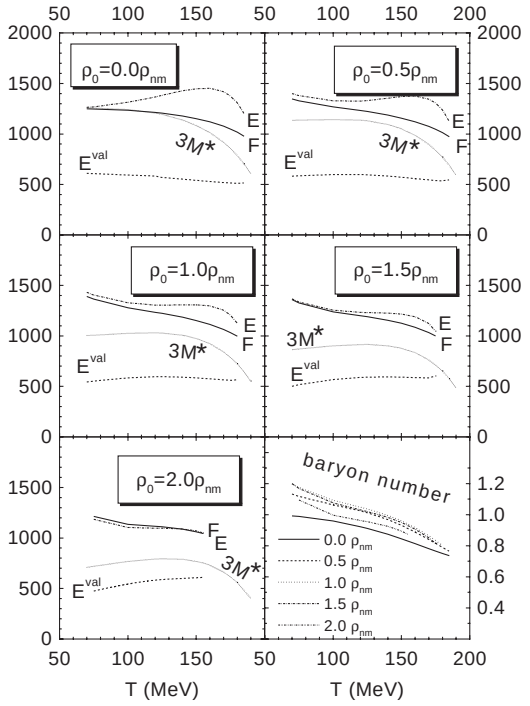

Fig. 3. Total internal (E) and free energy (F) of the soliton as a function of the medium temperature T for various medium densities ρ_0 ($\rho_{\rm nm} = 0.16\,{\rm fm}^{-3}$: normal nuclear density). The *dotted lines* show the contribution $E^{\rm val}$ of the valence quarks to the internal energy and the *dashed lines* represent the energy $3M^*$ of 3 free constituent quarks. The calculation was performed with a constituent quark mass $M = 420\,{\rm MeV}$ in vacuum. The *lowest right part* shows the baryon number B as a function of T for the densities considered in the other parts of the figure

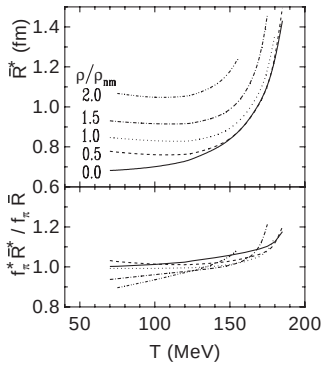

Fig. 4. Root mean-square radius $\bar{R}^*$ of the soliton as a function of the medium temperature T for various values of the medium density ρ_0 in units of the normal nuclear density $\rho_{\rm nm} = 0.16\,{\rm fm}^{-3}$ calculated for $M = 420\,{\rm MeV}$. The *lower part* shows the deviation from Brown-Rho scaling. $\bar{R}^*$ and f_π^* are radius and pion decay constant at given medium temperature T and density ρ_0 while $\bar{R}$ and f_π denote the corresponding values at $T = \rho_0 = 0$

problems will occur when calculating the moment of inertia in Sect. 5. That is why we tolerate a baryon number slightly different from one and do not introduce different chemical potentials ensuring that any local expectation value of the soliton vanishes asymptotically.

There is a promising method in the literature which might be applied to fix the baryon number of the soliton to one without changing the chemical potential. In [21] the regularized version of the baryon number in vacuum, which differs also from one, could be constrained after introducing the chiral radius field as an additional dynamical degree of freedom. In the center of the soliton, this radius field deviates noticeably from the chiral circle. Additionally, the constraint on the baryon number prevents the soliton with a space dependent radius field from collapsing. This method will be investigated in a forthcoming paper.

4 Energy and radius of the soliton

In this section we display and discuss energy, baryon number and r.m.s. radius of the soliton defined in Sect. 2. Figure 3 shows internal and free energy as a function of the medium temperature T for several densities ρ_0. While the internal energy represents the total energy which is necessary to generate the soliton the free energy disregards that part of the energy which is automatically delivered by the heat bath.

The first striking feature we want to mention is the relative independence of the valence quark energy on temperature and medium density, and hence on the constituent quark mass M^*. The latter determines the depth of the well in the solitonic σ field which binds the valence quarks. The decreasing depth at growing T and/or ρ_0 is nearly compensated by a larger radius of the self-consistently determined potential well with the result that the valence level is kept at an almost unchanged energy of roughly $500/3\,{\rm MeV}$. The solitonic solution of the equations of motion disappears if the valence level comes close to the top of the well in the σ field. Comparing total soliton energy with the mass of 3 free constituent quarks we notice that the soliton energy depends more weakly on T and ρ_0 than the constituent quark mass.

Comparing the free soliton energy with the results of [7] we notice differences up to several hundred MeV especially at larger medium density. They are to attribute to different assumptions concerning the occupation of the valence level in the homogeneous medium and to the two different chemical potentials used in [7]. On the other hand, our baryon number which decreases with increasing temperature superimposes the T dependence of the soliton energy. Dividing the free energy by the baryon number it exhibits a slight increase with increasing temperature.

The r.m.s. radii $\bar{R}^*$ (48) displayed in Fig. 4 indicate a swelling of the soliton when temperature and density increase. At low temperature the soliton swells roughly linearly with increasing medium density. The soliton at normal nuclear density is by roughly 20 percent larger than in vacuum. Above 125 MeV the r.m.s. radius grows

continuously towards the deconfinement transition. There are two different reasons for the modification of the soliton size in the medium: the increase of the radius of the self-consistent mean field and the polarization of the medium quarks around the soliton. The first effect is rather pronounced and nearly proportional to $1/M^*$. The polarization modifies the baryon density very slightly but at rather large distances from the center of the soliton and has therefore a noticeable influence on the mean-square radius. The effect is positive at lower temperatures and negative at high temperatures. It raises the dependence of the r.m.s. radius on the medium density and reduces its dependence on the temperature. A comparison with the r.m.s. radii obtained in [7] is difficult because of the finite baryon density outside the soliton which inevitably emerges in a model with two different chemical potentials. To get a finite soliton radius this part was obviously ignored. In contrast to [7] we get always a larger radius if the medium density increases for any temperature.

The lower part of Fig. 4 illustrates the deviation from the Brown-Rho scaling [22] which predicts $\bar{R}/\bar{R}^* \approx f_\pi^*/f_\pi$. Apart from the immediate vicinity of the deconfinement transition the deviation does not exceed 10 percent.

5 Quasi-classical energy corrections

The soliton considered so far exhibits several undesired properties which do not allow a direct comparison with the nucleon or other baryons. Due to the mean-field approximation the translational symmetry is violated and the soliton energy is contaminated by spurious center-of-mass motion. We estimate the spurious part of the soliton energy which is connected with quantum fluctuations around the artificially fixed position of the soliton by means of quasi-classical methods and subtract it from the total energy. The same is done for the rotational degrees of freedom where the restriction to hedgehog configurations introduces an alignment of the isospin of the soliton inducing spurious fluctuations as well. Moreover we introduce a collective rotation of the soliton as a whole in order to equip it with definite values of spin and isospin and add the corresponding rotational energy to the total soliton energy giving rise to a mass difference between nucleon and Δ isobar. Rotations in space and isospace are not independent of each other since the total isospin of the hedgehog soliton is directed opposite to its spin. Fluctuations and rotational energies in both spaces are equal and have to be considered only once. We perform our calculation in isospace which can simpler be treated.

The perturbative quasi-classical approach used for the determination of spurious translational and rotational contributions to the soliton energy has been adopted from low-energy nuclear physics where it is denoted as pushing and cranking approach [10], respectively. The same correction terms can be derived if one includes boosted and rotating meson fields in the stationary phase approximation, which leads to the effective action of the model [2].

First we consider fluctuations of the total soliton momentum $\boldsymbol{P} = \int \mathrm{d}^3\boldsymbol{r}\, q^\dagger(\boldsymbol{r})\, \boldsymbol{p}\, q(\boldsymbol{r})$ which are described by the dispersion

$$\left\langle\!\left\langle \left(\Delta \boldsymbol{P}\right)^2 \right\rangle\!\right\rangle \equiv \left\langle\!\left\langle \boldsymbol{P}^2 \right\rangle\!\right\rangle - \left\langle\!\left\langle \boldsymbol{P} \right\rangle\!\right\rangle^2 . \tag{49}$$

To evaluate expectation values of $\boldsymbol{P}$ and $\boldsymbol{P}^2$ we use the regularized version of the extended canonical quark potential (29-38) with $\kappa\mathcal{O} = \boldsymbol{v}\cdot\boldsymbol{p}$. It describes the grand canonical potential in a frame boosted with velocity $\boldsymbol{v}$ relative to the rest frame of the soliton. On the analogy of (33) the expectation value is given by

$$\begin{aligned} \left\langle\!\left\langle \boldsymbol{P} \right\rangle\!\right\rangle &= -\left.\frac{\partial \Omega_\Lambda^{\rm q}(T,\mu;\boldsymbol{v})}{\partial \boldsymbol{v}}\right|_{\boldsymbol{v}=\boldsymbol{0}} \\ &= -N_{\rm c} T \mathrm{Tr}_\Lambda \Big[\left(D(\mu)^{-1} - D_0(\mu)^{-1}\right) \boldsymbol{p} \Big] = 0 . \end{aligned} \tag{50}$$

It vanishes for any time-independent hamiltonian h. Squares like $\boldsymbol{P}^2$ of a one-body operator (28) can be decomposed into a one-body operator $\left[\boldsymbol{P}^2\right]_{(1)} = \int \mathrm{d}^3\boldsymbol{r}\, q^\dagger(\boldsymbol{r})\, \boldsymbol{p}^2\, q(\boldsymbol{r})$ and a normal ordered two-body operator $\left[\boldsymbol{P}^2\right]_{(2)}$. The expectation values of the latter can be expressed by the second derivative of the extended canonical potential (29) and the product of two one-body expectation values. We get

$$\left\langle\!\left\langle \boldsymbol{P}^2 \right\rangle\!\right\rangle = \left\langle\!\left\langle \left[\boldsymbol{P}^2\right]_{(1)} \right\rangle\!\right\rangle + \left\langle\!\left\langle \boldsymbol{P} \right\rangle\!\right\rangle^2 - T \left.\frac{\partial^2 \Omega_\Lambda^{\rm q}(T,\mu;\boldsymbol{v})}{\partial \boldsymbol{v}\cdot\partial \boldsymbol{v}}\right|_{\boldsymbol{v}=\boldsymbol{0}} . \tag{51}$$

Introducing the inertial mass tensor

$$\mathcal{M}_{ik}(T,\mu) = -\left.\frac{\partial^2 \Omega_\Lambda^{\rm q}(T,\mu;\boldsymbol{v})}{\partial v^i \partial v^k}\right|_{\boldsymbol{v}=\boldsymbol{0}} = \mathcal{M}(T,\mu)\,\delta_{ik} , \tag{52}$$

which is diagonal for spherically symmetric solitons and has identical matrix elements, we get for the dispersion (49)

$$\left\langle\!\left\langle (\Delta \boldsymbol{P})^2 \right\rangle\!\right\rangle = \left\langle\!\left\langle \left[\boldsymbol{P}^2\right]_{(1)} \right\rangle\!\right\rangle + 3T\mathcal{M} . \tag{53}$$

The minus sign in the mass definition (52) results from the anti-hermitian character of the euclidean velocity $\boldsymbol{v}$. Equation (52) defines the inertial soliton mass by the response of the grand canonical potential to a boost at fixed values of T and μ. Since the variation of Ω at fixed T and μ is equivalent to the variation of the free energy (22) at fixed T and baryon number B, and also equivalent to the variation of the internal energy (21) if B and entropy $S = -\partial\Omega/\partial T$ are fixed, we can rewrite (52) accordingly. However, the determination via Ω is the most appropriate one in our case since we have an explicit representation of the grand canonical potential on its variables T and μ. That is not the case for internal (21) and free energy (22).

In the non-relativistic limit, the dispersion (53) corresponds to the following energy of the translational fluctuations of the soliton

$$E_{\rm trans}^{\rm fl} = \frac{\left\langle\!\left\langle (\Delta \boldsymbol{P})^2 \right\rangle\!\right\rangle}{2\mathcal{M}} = \frac{\left\langle\!\left\langle \left[\boldsymbol{P}^2\right]_{(1)} \right\rangle\!\right\rangle}{2\mathcal{M}} + \frac{3}{2}T . \tag{54}$$

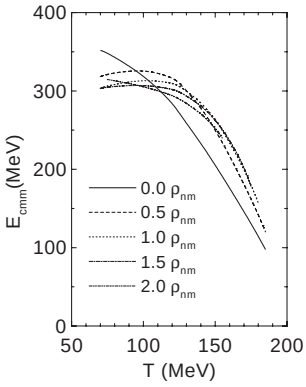

Fig. 5. Energy $E_{\rm cmm}=\langle\!\langle\left[\boldsymbol{P}^2\right]_{(1)}\rangle\!\rangle/2\mathcal{M}$ of the center-of-mass motion as a function of the medium temperature T for various values of the density in units of the normal nuclear density $\rho_{\rm nm}=0.16\,{\rm fm}^3$ and $M=420\,{\rm MeV}$

While the second term describes thermal fluctuations of the soliton mass center in a medium with $T>0$ the first term represents the energy of the unphysical quantum fluctuations of the mass center which has to be eliminated from the total soliton energy. Figure 5 displays this energy as a function of medium temperature and density. The main contribution to the center-of-mass energy stems from the valence quarks which are confined by the well in the mean field. The calculated reduction of $E_{\rm cmm}$ with increasing temperature can be explained by the swelling of the soliton in accordance with Heisenberg's uncertainty principle. But there is only a loose relation between center-of-mass energy and r.m.s. radius (Fig. 4) since the soliton radius incorporates not only the modified mean field but also the medium polarization.

After an equivalent consideration for the dispersion of the isospin operator $\boldsymbol{T}=\int{\rm d}^3\boldsymbol{r}\,q^\dagger(\boldsymbol{r})\,\boldsymbol{t}\,q(\boldsymbol{r})$, where $\boldsymbol{t}=\boldsymbol{\tau}/2$ denotes the single-particle isospin operator, we get by means of the generating function (29) with $\kappa\mathcal{O}=\boldsymbol{\omega}\cdot\boldsymbol{t}$

$$E^{\rm fl}_{\rm rot}=\frac{\langle\!\langle(\Delta\boldsymbol{T})^2\rangle\!\rangle}{2\mathcal{J}}=\frac{\langle\!\langle\left[\boldsymbol{T}^2\right]_{(1)}\rangle\!\rangle}{2\mathcal{J}}+\frac{3}{2}T \tag{55}$$

for the energy of the rotational fluctuations with the isorotational moment of inertia

$$\mathcal{J}_{ik}(T,\mu)=-\left.\frac{\partial^2\Omega^{\rm q}_\Lambda(T,\mu;\boldsymbol{\omega})}{\partial\omega^i\partial\omega^k}\right|_{\boldsymbol{\omega}=\boldsymbol{0}}=\mathcal{J}(T,\mu)\,\delta_{ik}\,. \tag{56}$$

The moment of inertia is diagonal for symmetry reasons and has identical diagonal elements. The energy of a soliton rotating semi-classically in isospace with isospin quantum number $\mathcal{T}$ and moment of inertia $\mathcal{J}$ is given by

$$E^{\mathcal{T}}_{\rm crank}=\frac{\mathcal{T}(\mathcal{T}+1)}{2\mathcal{J}}\,. \tag{57}$$

The corrected energy of a soliton with isospin $\mathcal{T}$ and spin $J=\mathcal{T}$ is obtained by subtracting the energy of the spurious quantum fluctuations (first term in (54, 55)) and adding the cranking energy (57) to the soliton energy (21)

$$E^{\mathcal{T}}_{\rm corr}=E-\frac{\langle\!\langle\left[\boldsymbol{P}^2\right]_{(1)}\rangle\!\rangle}{2\mathcal{M}}-\frac{\langle\!\langle\left[\boldsymbol{T}^2\right]_{(1)}\rangle\!\rangle}{2\mathcal{J}}+\frac{\mathcal{T}(\mathcal{T}+1)}{2\mathcal{J}}\,. \tag{58}$$

The difference between the masses of Δ isobar ($\mathcal{T}=3/2$) and nucleon ($\mathcal{T}=1/2$) is then given by

$$\Delta E_{\Delta N}\equiv E^{\mathcal{T}=3/2}_{\rm corr}-E^{\mathcal{T}=1/2}_{\rm corr}=\frac{3}{2\mathcal{J}}\,. \tag{59}$$

Evaluating the corrected soliton energy (58) the expectation value of the one-body operator $\left[\boldsymbol{P}^2\right]_{(1)}$ has to be calculated numerically using (33–38) with $\mathcal{O}=\boldsymbol{p}^2$ and the regularized sea contribution (37). The expectation value of the corresponding isospin operator can analytically be determined since the single-particle expectation values of $\boldsymbol{t}^2$ are the same for all quark levels independently of the meson fields $\big(\langle\alpha|\boldsymbol{t}^2|\alpha\rangle=\langle\alpha^0|\boldsymbol{t}^2|\alpha^0\rangle=1/2(1/2+1)\big)$. Hence most of the contributions to the expectation value cancel out each other and we get

$$\langle\!\langle\left[\boldsymbol{T}^2\right]_{(1)}\rangle\!\rangle=N_{\rm c}B\,\frac{1}{2}\left(\frac{1}{2}+1\right)=\frac{9}{4}\,B\,. \tag{60}$$

The inertial parameters $\mathcal{M}$ and $\mathcal{J}$ will be determined in the subsequent subsections.

5.1 Inertial soliton mass

In this subsection, we show that the inertial mass (52) of the soliton is identical with its internal energy (21) and need not be calculated separately

$$\mathcal{M}=E^{\rm m}+E^{\rm q,sea}_\Lambda+E^{\rm q,med}=E\,. \tag{61}$$

Assuming spherical symmetry we get by means of the derivations in appendix B, which result in (B.11, B.23), for the inertial soliton mass

$$\begin{aligned}\mathcal{M}&=\frac{1}{3}\sum_i\mathcal{M}_{ii}=-\frac{1}{3}\left.\frac{\partial^2\Omega^{\rm q}_\Lambda(T,\mu;\boldsymbol{v})}{\partial\boldsymbol{v}\cdot\partial\boldsymbol{v}}\right|_{\boldsymbol{v}=\boldsymbol{0}}\\&=\mathcal{M}^{\rm sea}_\Lambda+\mathcal{M}^{\rm med}\end{aligned} \tag{62}$$

with

$$\begin{aligned}\mathcal{M}^{\rm sea}_\Lambda&\equiv-\frac{1}{3}\left.\frac{\partial^2\Omega^{\rm q,sea}_\Lambda(\boldsymbol{v})}{\partial\boldsymbol{v}\cdot\partial\boldsymbol{v}}\right|_{\boldsymbol{v}=\boldsymbol{0}}\\&=-N_{\rm c}\int\limits_{1/\Lambda^2}^{\infty}{\rm d}s\lim_{T\to0}T{\rm Tr}\Big[{\rm e}^{-sA(0)}\\&\quad\times\Big(\frac{\boldsymbol{p}^2}{3}+\partial_\tau^2+\frac{\rm i}{6}\boldsymbol{\gamma}\cdot\boldsymbol{\nabla}(\sigma+{\rm i}\gamma_5\boldsymbol{\tau}\cdot\hat{\boldsymbol{r}}\,\pi)\Big)-{\rm e}^{-sA_0(0)}\partial_\tau^2\Big]\end{aligned} \tag{63}$$

and

$$\mathcal{M}^{\rm med} \equiv -\frac{1}{3}\left.\frac{\partial^2\Omega^{\rm q,med}(T,\mu;\boldsymbol{v})}{\partial\boldsymbol{v}\cdot\partial\boldsymbol{v}}\right|_{\boldsymbol{v}=\boldsymbol{0}} \tag{64}$$
$$= -N_{\rm c}T{\rm Tr}\Big[A(\mu)^{-1}\Big(\frac{\boldsymbol{p}^2}{3}+\partial_\tau^2+\frac{\rm i}{6}\boldsymbol{\gamma}\cdot\boldsymbol{\nabla}(\sigma+{\rm i}\gamma_5\boldsymbol{\tau}\cdot\hat{\boldsymbol{r}}\,\pi)\Big) - A_0(\mu)^{-1}\partial_\tau^2\Big]$$
$$+N_{\rm c}\lim_{T\to0}T{\rm Tr}\Big[A(0)^{-1}\Big(\frac{\boldsymbol{p}^2}{3}+\partial_\tau^2+\frac{\rm i}{6}\boldsymbol{\gamma}\cdot\boldsymbol{\nabla}(\sigma+{\rm i}\gamma_5\boldsymbol{\tau}\cdot\hat{\boldsymbol{r}}\,\pi)\Big) - A_0(0)^{-1}\partial_\tau^2\Big]$$
$$-N_{\rm c}T{\rm Tr}\Big[A(\mu)^{-1}\mu\Big((h-\mu)+\frac{\rm i}{3}\boldsymbol{r}\cdot[h,\boldsymbol{p}]\Big) - A_0(\mu)^{-1}\mu(h_0-\mu)\Big]$$

with $A_{(0)}(\mu)$ defined in (B.1). Now we exploit the invariance of the potential Ω with respect to an arbitrary variation of the meson fields σ and π around the stationary point in accordance with the equation of motion (18). A variation which is in accordance with both the spherical hedgehog symmetry and the chiral circle respecting the boundary conditions $\delta\sigma=0$ and $\delta\pi=0$ at small and large separations from the center of the soliton is given by

$$\delta\sigma = \epsilon\, r^k\partial_k\sigma \qquad \text{and} \qquad \delta\boldsymbol{\pi} = \epsilon\, r^k\partial_k\boldsymbol{\pi} = \epsilon\, r^k\partial_k(\hat{\boldsymbol{r}}\,\pi) \tag{65}$$

with an infinitesimal variation parameter ϵ. Such a variation of the meson fields gives rise to the following changes $\delta\Omega^{\rm m}, \delta\Omega_\Lambda^{\rm q,sea}$ and $\delta\Omega^{\rm q,med}$ in the mesonic and quark contributions to the grand canonical potential (10)

$$\frac{\delta\Omega^{\rm m}}{\epsilon} = -\frac{m}{G}\int{\rm d}^3\boldsymbol{r}\,\frac{\delta\sigma(r)}{\epsilon} \tag{66}$$
$$= -\frac{m}{G}\int{\rm d}^3\boldsymbol{r}\; r^k\partial_k\sigma = 3\frac{m}{G}\int{\rm d}^3\boldsymbol{r}\,(\sigma-\sigma_0) = -3\Omega^{\rm m}\,,$$

$$\delta\Omega_\Lambda^{\rm q,sea} = -\frac{N_{\rm c}}{2}\int\limits_{1/\Lambda^2}^{\infty}{\rm d}s\lim_{T\to0}T{\rm Tr}\left[{\rm e}^{-sA(0)}\,\delta h^2\right]\,, \tag{67}$$

$$\delta\Omega^{\rm q,med} = -\frac{N_{\rm c}}{2}T{\rm Tr}\left[A(\mu)^{-1}\,\delta(h-\mu)^2\right] + \frac{N_{\rm c}}{2}\lim_{T\to0}T{\rm Tr}\left[A(0)^{-1}\delta h^2\right] \tag{68}$$

with

$$\frac{\delta h}{\epsilon} = \beta\left(\frac{\delta\sigma}{\epsilon}+{\rm i}\gamma_5\boldsymbol{\tau}\cdot\frac{\delta\boldsymbol{\pi}}{\epsilon}\right) = \beta\,\boldsymbol{r}\cdot\boldsymbol{\nabla}(\sigma+{\rm i}\gamma_5\boldsymbol{\tau}\cdot\hat{\boldsymbol{r}}\,\pi) \tag{69}$$
$$= -{\rm i}\boldsymbol{r}\cdot[h,\boldsymbol{p}] = \boldsymbol{\alpha}\cdot\boldsymbol{p}-{\rm i}[h,\boldsymbol{r}\cdot\boldsymbol{p}]\,,$$

$$\frac{\delta h^2}{\epsilon} = \left\{h,\frac{\delta h}{\epsilon}\right\} \tag{70}$$
$$= 2\boldsymbol{p}^2+{\rm i}\boldsymbol{\gamma}\cdot\boldsymbol{\nabla}(\sigma+{\rm i}\gamma_5\boldsymbol{\tau}\cdot\hat{\boldsymbol{r}}\,\pi)-{\rm i}\left[h^2,\boldsymbol{r}\cdot\boldsymbol{p}\right]\,,$$

$$\delta(h-\mu)^2 = \delta h^2 - 2\mu\delta h\,. \tag{71}$$

Now we introduce first $\delta h, \delta h^2$ and $\delta(h-\mu)^2$ and then $\delta\Omega_\Lambda^{\rm q,sea}$ and $\delta\Omega^{\rm q,med}$ into (62-64) and get by means of the equation of motion (18) and the variation (66) of $\Omega^{\rm m}$

$$\mathcal{M} = \Omega^{\rm m} - N_{\rm c}\int\limits_{1/\Lambda^2}^{\infty}{\rm d}s\lim_{T\to0}T{\rm Tr}\Big[\Big({\rm e}^{-sA(0)}-{\rm e}^{-sA_0(0)}\Big)\partial_\tau^2\Big]$$
$$-N_{\rm c}T{\rm Tr}\Big[A(\mu)^{-1}\left(\partial_\tau^2+\mu(h-\mu)\right) - A_0(\mu)^{-1}\left(\partial_\tau^2+\mu(h_0-\mu)\right)\Big] \tag{72}$$
$$+N_{\rm c}\lim_{T\to0}T{\rm Tr}\Big[\Big(A(0)^{-1}-A_0(0)^{-1}\Big)\partial_\tau^2\Big]\,.$$

The agreement of $\mathcal{M}$ with the internal energy (21) can now be established by means of (A.10–A.13) by comparing the various terms in (72) with the components (23–25) of the internal energy.

The equivalence of inertial soliton mass and total mean-field energy is by far not trivial despite the Lorentz-invariance of the initial NJL Lagrangian. The approximations, the particular regularization scheme applied only on the Dirac-sea contribution and the presence of the medium might disturb the equivalence of inertial mass and total internal energy.

5.2 Iso-rotational moment of inertia and Δ-nucleon mass splitting

The iso-rotational moment

$$\mathcal{J} = \frac{1}{3}\sum_i\mathcal{J}_{ii} = -\frac{1}{3}\left.\frac{\partial^2\Omega_\Lambda^{\rm q}(T,\mu;\boldsymbol{\omega})}{\partial\boldsymbol{\omega}\cdot\partial\boldsymbol{\omega}}\right|_{\boldsymbol{\omega}=\boldsymbol{0}} \tag{73}$$
$$= \mathcal{J}_\Lambda^{\rm sea}+\mathcal{J}^{\rm med}$$

consists of the components

$$\mathcal{J}_\Lambda^{\rm sea} \equiv -\frac{1}{3}\left.\frac{\partial^2\Omega_\Lambda^{\rm q,sea}(\boldsymbol{\omega})}{\partial\boldsymbol{\omega}\cdot\partial\boldsymbol{\omega}}\right|_{\boldsymbol{\omega}=\boldsymbol{0}} \tag{74}$$
$$= \frac{N_{\rm c}}{4}\sum_{\alpha\beta}\left[\frac{R_{\mathcal{J}}(\varepsilon_\alpha,\varepsilon_\beta;\Lambda)}{\varepsilon_\alpha-\varepsilon_\beta}\,\langle\,\alpha\,|\,\tau_3\,|\,\beta\,\rangle\,\langle\,\beta\,|\,\tau_3\,|\,\alpha\,\rangle - \frac{R_{\mathcal{J}}(\varepsilon_\alpha^0,\varepsilon_\beta^0;\Lambda)}{\varepsilon_\alpha^0-\varepsilon_\beta^0}\langle\alpha^0|\tau_3|\beta^0\rangle\langle\beta^0|\tau_3|\alpha^0\rangle\right]$$

with

$$R_{\mathcal{J}}(\varepsilon_\alpha,\varepsilon_\beta;\Lambda) \tag{75}$$
$$= \frac{\Lambda}{\sqrt{\pi}}\frac{{\rm e}^{-\varepsilon_\beta^2/\Lambda^2}-{\rm e}^{-\varepsilon_\alpha^2/\Lambda^2}}{\varepsilon_\beta+\varepsilon_\alpha}+\frac{1}{2}\Big({\rm erf_c}(\varepsilon_\alpha/\Lambda)-{\rm erf_c}(\varepsilon_\beta/\Lambda)\Big)$$

and

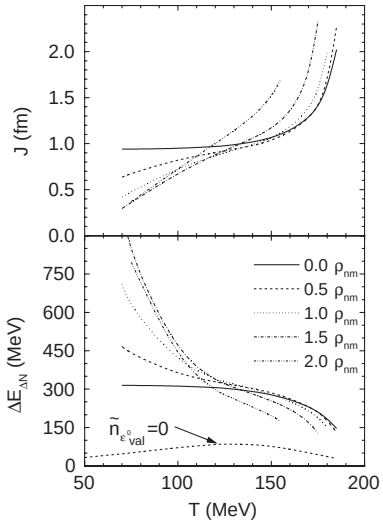

Fig. 6. Moment of inertia $\mathcal{J}$ (*upper part*) and Δ-nucleon mass splitting $\Delta E_{\Delta N}$ (*lower part*) as a function of the medium temperature T for various values ρ_0 of the density and constituent quark mass $M = 420\,\mathrm{MeV}$ in vacuum. The *lowest line* in the lower part shows the splitting for $\rho_0 = 0.5\rho_{\mathrm{nm}}$ obtained with the assumption that the valence level is empty in the homogeneous medium

$$\mathcal{J}^{\mathrm{med}} \equiv -\frac{1}{3}\,\frac{\partial^2 \Omega^{\mathrm{q,med}}(T,\mu;\boldsymbol{\omega})}{\partial\boldsymbol{\omega}\cdot\partial\boldsymbol{\omega}}\bigg|_{\boldsymbol{\omega}=\mathbf{0}} \tag{76}$$

$$= -N_{\mathrm{c}} T \mathrm{Tr}\Big[D(\mu)^{-1} t_3 D(\mu)^{-1} t_3 - D_0(\mu)^{-1} t_3 D_0(\mu)^{-1} t_3\Big]$$

$$+N_{\mathrm{c}} \lim_{T\to 0} T\mathrm{Tr}\Big[D(0)^{-1} t_3 D(0)^{-1} t_3 - D_0(0)^{-1} t_3 D_0(0)^{-1} t_3\Big]$$

$$= \frac{N_{\mathrm{c}}}{4}\sum_{\alpha\beta}\Bigg[\frac{\tilde{n}_{\varepsilon_\beta}-\tilde{n}_{\varepsilon_\alpha}}{\varepsilon_\alpha-\varepsilon_\beta}\,\langle\,\alpha\,|\,\tau_3\,|\,\beta\,\rangle\,\langle\,\beta\,|\,\tau_3\,|\,\alpha\,\rangle$$

$$- \frac{\tilde{n}_{\varepsilon^0_\beta}-\tilde{n}_{\varepsilon^0_\alpha}}{\varepsilon^0_\alpha-\varepsilon^0_\beta}\big\langle\alpha^0\big|\tau_3\big|\beta^0\big\rangle\big\langle\beta^0\big|\tau_3\big|\alpha^0\big\rangle\Bigg]\,.$$

While the sea component (74) has been derived in [23] the medium contribution (76) is obtained by means of (6, 7, A.1, A.2, A.8, A.9). Since the single-particle hamiltonian h_0 of the homogeneous medium commutes with τ_3 only diagonal elements with $\alpha^0 = \beta^0$ contribute to the corresponding terms in the inertial momenta (74, 76). Because of $\lim_{\varepsilon'\to\varepsilon} R_{\mathcal{J}}(\varepsilon,\varepsilon';\Lambda)/(\varepsilon-\varepsilon') = 0$ these terms vanish in (74) and the homogeneous medium does not contribute to sea component of the inertial moment. That is not true for a calculation in the discrete basis [20] with boundary conditions depending on the superspin quantum number. Here we have numerically to determine the inertial moment of the homogeneous medium and to subtract from the moment of the solitonic configuration.

Figure 6 illustrates the moment of inertia as a function of medium temperature and density. At vanishing density, the moment is nearly constant and increases remarkably only in the neighborhood of the critical temperature at 185 MeV. At finite medium density, the increase starts earlier. The main contribution to the moment of inertia comes from transition matrix elements between the valence level and an unoccupied level in its vicinity. At finite density, the levels around the valence level are sufficiently occupied by quarks representing the medium and the moment of inertia is remarkably reduced in comparison to the vacuum (Pauli blocking). The resulting moment of inertia is very small and the ΔN mass splitting (Fig. 6, lower part) is huge at low temperature and finite density. This is an obvious shortcoming of the model describing the medium as gas of constituent quarks. In a more realistic picture, the medium quarks should be bound in solitons and the corresponding transition matrix elements are not blocked to that degree. At higher temperature, the probability of finding a hole close to the valence level increases. Here the blocking effect diminishes. If one keeps the valence level of the homogeneous medium free ($\tilde{n}_{\varepsilon^0_{\mathrm{val}}} = 0$) as in [7,9] one gets big transition matrix elements to that level, and the moment of inertia is huge. The resulting ΔN splitting is negligibly small already at half of normal nuclear density (lowest line in Fig. 6) and further decreases if the density grows. That is another reason why we discarded this method of tailoring a $B = 1$ soliton.

The quasi-classical energy corrections in (58) represent approximations to the first terms in an $1/N_{\mathrm{c}}$ expansion. While the quantum fluctuations behave like $(1/N_{\mathrm{c}})^0$ the cranking term is proportional to $1/N_{\mathrm{c}}$. So it is not surprising that the mass shift at $\rho_0 = 0$ obtained in our approach exhibits a similar dependence on T as the shift evaluated in heavy baryon chiral perturbation theory (HBχPT) using a $1/N_{\mathrm{c}}$ expansion [24]. The shift is negative for nucleons and positive for Δ isobars and has the same absolute value in our approach apart from a term which is proportional to the deviation of the baryon number from one. The identity of the absolute values of the mass shifts for nucleon and Δ isobar is the result of the restriction to 2 quark flavors in contrast to the HBχPT calculation which includes strange quarks. At $T \approx 130\,\mathrm{MeV}$ the ΔN splitting is reduced by only 5% in comparison to 20% in [24]. Again a partial blocking of quark levels in the neighborhood of the valence level prevents a larger moment of inertia and reduces the decrease of the ΔN splitting at finite temperature.

6 Energy of the nucleon

In Fig. 7, we display the corrected internal energy (58) and the corresponding free energy in dependence on temperature and density of the medium for nucleons ($\mathcal{T} = 1/2$). In the considered region, the baryon number varies between 1.2 and 0.8 as displayed in the lower right corner of Fig. 3. To estimate the effect of the varying baryon number we display the energy per baryon number on the right panel of Fig. 7. We see that the variation in the baryon number has only a moderate influence on the corrected soliton energy. The behavior of the soliton energy in dependence on temperature and density differs remarkably from the corresponding behavior of free constituent quarks (dotted

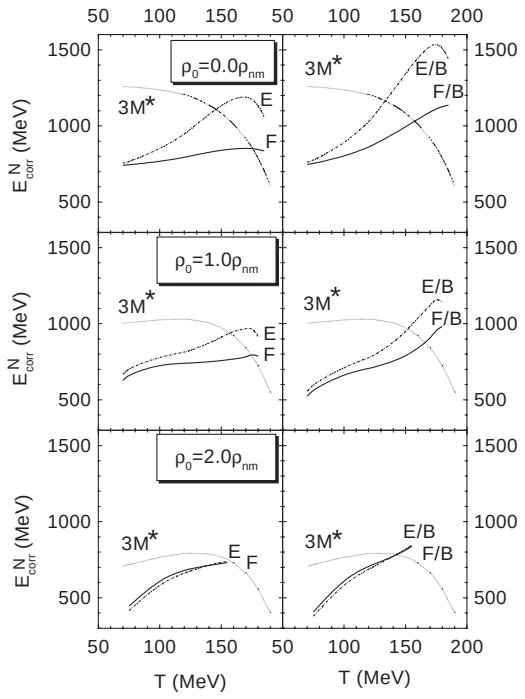

Fig. 7. Total corrected internal (E) and free energy (F) of the nucleon as a function of the medium temperature T for 3 values of the medium densities ρ_0 and constituent quark mass $M = 420$ MeV in vacuum. The *left panel* shows the corrected energies for particles with the varying baryon numbers displayed in Fig. 3. The corresponding energies per baryon number are shown on the *right panel*

lines). While constituent quarks get lighter with increasing temperature the soliton gets heavier. The dependence on the medium density is weaker for solitons than for constituent quarks.

The increase of the nucleon mass is mainly due to the reduction of the center-of-mass energy (Fig. 5) which shrinks from 350 MeV at $T = 0$ to 100 MeV close to the critical temperature. This has to be taken into account if one compares with calculations which do not consider this spurious energy. A slight decrease of the nucleon mass at higher temperature as e. g. observed in [25] is changed into an increase by means of the center-of-mass energy. Center-of-mass corrections do also reduce the density dependence of the nucleon mass at low temperatures.

We should mention that the calculated nucleon mass in vacuum is by roughly 200 MeV smaller than the experimental value. This is an obvious shortcoming of the simple effective model and the approximations applied in the course of the evaluation. For that reason the model is preferably used for the evaluation of the splitting between the masses of different baryons. In that sense we do not consider the absolute masses but their variation in dependence on temperature and density. Furthermore we use the experimental Δ-nucleon mass-splitting in vacuum in order to fix the only free parameter of the model - the constituent quark mass in vacuum - to a value of 420 MeV .

7 Conclusions

We investigated the properties of a two-flavor NJL soliton which is embedded in a medium of constituent quarks with self-consistently determined constituent mass. Energy and mass of the soliton are determined in mean-field approximation with the restriction to hedgehog configurations and to the chiral circle. To get a solitonic solution of the corresponding equations of motion we have to fix the occupation probability of the valence level independently of the thermodynamical parameters of the medium. Otherwise the soliton dissolves below 100 MeV already at densities below the normal nuclear density. The expected critical values of medium temperature and density are obtained with the assumption that the occupation probability of the valence level equals to one, the same value as assumed for the soliton in vacuum.

Through lack of confinement the model does not allow the construction of a localized soliton with fixed baryon number as soon as medium temperature or density differ from zero. Keeping the baryonic charge confined within a finite radius around the soliton the baryon number of the self-consistent field configuration varies between 0.8 and 1.2 in dependence on temperature and density. Fixing the baryon number to a definite value by means of a chemical potential which differs from the chemical potential of the medium a part of solitonic baryon charge is uniformly distributed over the whole space. This is an obvious contradiction to the definition of a soliton.

To remove spurious contributions to the mean-field energy and to equip the soliton with the quantum numbers of nucleon or Δ isobar we adopted the quasi-classical pushing and cranking approaches. The resulting energy corrections are determined by inertial parameters describing the response of the soliton as a whole with respect to a translation or rotation. We found the nontrivial result that the inertial mass in the medium is identical with the internal energy of the soliton. The rotational moment of inertia was determined numerically.

It has turned out that the description of the medium as a non-interacting gas of constituent quarks moving in the solitonic mean field overestimates the effect of the medium on the soliton. In particular, the expected decrease of the ΔN splitting at increasing temperature and density is remarkably reduced by the quarks of the medium. At lower temperatures, the Pauli blocking of low lying quark levels by medium quarks dominates the behavior of such quantities which are described by transition matrix elements between different quark levels. It overcompensates, for instance, the influence of the swelling effect on the moment of inertia. Instead of increasing the moment of inertia decreases with increasing medium density.

As a result of its internal structure, which is generated by a self-consistently determined mean field, the behavior of the soliton energy in dependence on temperature and density deviates remarkably from the corresponding behavior of the constituent quark mass. The scaling property between both quantities is noticeably disturbed since the influence of the changed constituent mass (depth of the well in the mean field) on the soliton energy is ac-

companied by an variation of the size of the well in the self-consistent mean field.

After subtracting translational and rotational corrections the discrepancy gets even more pronounced since translational and rotational corrections decrease with increasing temperature and density. As a result the soliton mass increases with increasing temperature while the constituent mass decreases.

The swelling effect of the soliton in dependence on medium temperature and density is well pronounced. It does not only correspond to the increase of the radius of the self-consistent mean field but is also related to the polarization of the medium in the neighborhood of the soliton. The latter intensifies the swelling with increasing medium density but reduces the dependence on temperature.

The authors would like to thank K. Goeke, Ch. V. Christov and J. Berger for numerous helpful discussions and for their warm hospitality. R. W. is indebted to D. Ebert, R. Alkofer, H. Weigel and H. W. Barz for many helpful discussions and comments. M. S. thanks for the warm hospitality of the University of Rostock, in particular D. Blaschke as well as G. Soff, E. E. Kolomeitsev, A. Pfitzner and F. Creutzburg for helpful discussions.

Appendix

A Operator traces

Evaluating the trace Tr of an operator $\mathcal{O}(\partial_\tau, h)$ containing the differential operator ∂_τ and the time-independent operator h, which includes functional trace with anti-periodic boundary conditions in the euclidean time-interval $[0, 1/T]$ and traces tr over Dirac and Pauli matrices, we use the representation

$$\begin{aligned}\mathrm{Tr}\mathcal{O}(\partial_\tau,h) &= \int_0^{1/T}\mathrm{d}\tau\int\mathrm{d}^3\boldsymbol{r}\;\mathrm{tr}\,\langle\,\boldsymbol{r}\tau\,|\,\mathcal{O}(\partial_\tau,h)\,|\,\boldsymbol{r}\tau\,\rangle \qquad (A.1)\\ &= \sum_\alpha\sum_{n=-\infty}^{+\infty}\mathcal{O}(\mathrm{i}\omega_n,\varepsilon_\alpha)\end{aligned}$$

with the eigenvalues ε_α of h and the Matsubara frequencies $\omega_n = (2n+1)\pi T$. At $T\to 0$, the sum over n has to be replaced by an integral

$$\lim_{T\to0} T\mathrm{Tr}\mathcal{O}(\partial_\tau,h) = \sum_\alpha\int_{-\infty}^{+\infty}\frac{\mathrm{d}\omega}{2\pi}\,\mathcal{O}(\mathrm{i}\omega,\varepsilon_\alpha)\,. \qquad (A.2)$$

Within Schwinger's proper-time regularization scheme the regularized trace of the logarithm of a positively definite single-particle operator $\mathcal{O}$ at $T\to 0$ is given by

$$\begin{aligned}\lim_{T\to0} T\mathrm{Tr}_\Lambda\ln\mathcal{O}(\partial_\tau,h) &= -\int_{1/\Lambda^2}^{\infty}\frac{\mathrm{d}s}{s}\lim_{T\to0}T\mathrm{Tr}\,\mathrm{e}^{-s\mathcal{O}(\partial_\tau,h)}\\ &= -\int_{1/\Lambda^2}^{\infty}\frac{\mathrm{d}s}{s}\sum_\alpha\int_{-\infty}^{+\infty}\frac{\mathrm{d}\omega}{2\pi}\,\mathrm{e}^{-s\mathcal{O}(\mathrm{i}\omega,\varepsilon_\alpha)}\,. \qquad (A.3)\end{aligned}$$

When calculating traces such as in (A.1, A.2) we use the relations

$$\begin{aligned}&T\sum_{n=-\infty}^{+\infty}\Big[\ln\left(\omega_n^2+a^2\right)-\ln\left(\omega_n^2+b^2\right)\Big] \qquad (A.4)\\ &\quad= a-b+2T\ln\left(1+\mathrm{e}^{-a/T}\right)-2T\ln\left(1+\mathrm{e}^{-b/T}\right)\\ &\quad\overset{T\to0}{\longrightarrow}\int_{-\infty}^{+\infty}\frac{\mathrm{d}\omega}{2\pi}\Big[\ln\left(\omega^2+a^2\right)-\ln\left(\omega^2+b^2\right)\Big]\\ &\quad= |a|-|b| \qquad (A.5)\end{aligned}$$

and

$$T\sum_{n=-\infty}^{+\infty}\frac{1}{\mathrm{i}\omega_n+a} = \frac{1}{2}-\frac{1}{1+\mathrm{e}^{a/T}} \qquad (A.6)$$

$$\overset{T\to0}{\longrightarrow}\int_{-\infty}^{+\infty}\frac{\mathrm{d}\omega}{2\pi}\,\frac{1}{\mathrm{i}\omega+a} = \frac{\mathrm{sign}(a)}{2}\,. \qquad (A.7)$$

Evaluating products of two thermal propagators we use

$$\begin{aligned}&T\sum_{n=-\infty}^{+\infty}\frac{1}{\mathrm{i}\omega_n+a}\,\frac{1}{\mathrm{i}\omega_n+b} \qquad (A.8)\\ &\quad= \frac{T}{b-a}\sum_{n=-\infty}^{+\infty}\left[\frac{1}{\mathrm{i}\omega_n+a}-\frac{1}{\mathrm{i}\omega_n+b}\right]\\ &\quad= \frac{1}{a-b}\left[\frac{1}{1+\mathrm{e}^{a/T}}-\frac{1}{1+\mathrm{e}^{b/T}}\right]\\ &\quad\overset{T\to0}{\longrightarrow}\frac{1}{a-b}\Big[\Theta(-a)-\Theta(-b)\Big] = \frac{\mathrm{sign}(a)-\mathrm{sign}(b)}{2(b-a)}\,. \qquad (A.9)\end{aligned}$$

The following identities for traces of the operators (B.1) can be proven by means of the representations (A.1–A.3)

$$\int_{1/\Lambda^2}^{\infty}\mathrm{d}s\,\lim_{T\to0}T\mathrm{Tr}\Big[\mathrm{e}^{-sA(0)}\,\partial_\tau^2\Big] = \frac{1}{2}\lim_{T\to0}T\mathrm{Tr}_\Lambda\ln A(0)\,, \qquad (A.10)$$

$$\mathrm{Tr}\Big[A(\mu)^{-1}\partial_\tau^2\Big] = -\frac{T}{2}\frac{\partial}{\partial T}\mathrm{Tr}\ln A(\mu)\,, \qquad (A.11)$$

$$\mathrm{Tr}\Big[A(\mu)^{-1}\mu(h-\mu)\Big] = -\frac{\mu}{2}\frac{\partial}{\partial\mu}\mathrm{Tr}\ln A(\mu)\,, \qquad (A.12)$$

$$\lim_{T\to0}T\mathrm{Tr}\Big[A(\mu)^{-1}\partial_\tau^2\Big] = \frac{1}{2}\lim_{T\to0}T\mathrm{Tr}\ln A(\mu)\,. \qquad (A.13)$$

In some of the equations above we have neglected an infinitely large constant which vanishes if one considers the difference between two traces.

B Evaluation of the mass tensor

Evaluating the mass tensor (52) we introduce the hermitian operators

$$A_{(0)}(\mu) \equiv D_{(0)}(\mu)^\dagger\, D_{(0)}(\mu) = -\partial_\tau^2 + (h_{(0)} - \mu)^2 \quad \text{(B.1)}$$

and

$$\begin{aligned} A_{(0)}(\mu;\boldsymbol{v}) &\equiv D_{(0)}(\mu;\boldsymbol{v})^\dagger\, D_{(0)}(\mu;\boldsymbol{v}) \quad \text{(B.2)} \\ &= A_{(0)}(\mu) + B^i_{(0)} v^i - (\boldsymbol{v}\cdot\boldsymbol{p})^2\,, \end{aligned}$$

with $D_{(0)}(\mu)$ from (6, 7), $D_{(0)}(\mu;\boldsymbol{v})$ from (30) with $\kappa\mathcal{O} = \boldsymbol{v}\cdot\boldsymbol{p}$, and with the operators

$$\begin{aligned} B^i &\equiv \frac{\partial}{\partial v^i} A(\mu;\boldsymbol{v})\bigg|_{\boldsymbol{v}=\mathbf{o}} = p^i D(\mu) - D(\mu)^\dagger p^i \quad \text{(B.3)} \\ &= 2p^i\partial_\tau - \big[h, p^i\big] = 2p^i\partial_\tau - \mathrm{i}\beta\,\partial_i\left[\sigma(\boldsymbol{r}) + \mathrm{i}\gamma_5\boldsymbol{\tau}\cdot\boldsymbol{\pi}(\boldsymbol{r})\right]\,, \end{aligned}$$

$$\begin{aligned} B^i_0 &\equiv \frac{\partial}{\partial v^i} A_0(\mu;\boldsymbol{v})\bigg|_{\boldsymbol{v}=\mathbf{o}} \quad \text{(B.4)} \\ &= p^i D_0(\mu) - D_0(\mu)^\dagger p^i = 2p^i\partial_\tau\,, \end{aligned}$$

which are independent of the chemical potential μ. Here we consider more general meson fields $\sigma(\boldsymbol{r})$ and $\boldsymbol{\pi}(\boldsymbol{r})$ which are not necessarily restricted to hedgehog configurations and to the chiral circle. The commutator $\big[h, p^i\big]$ in (B.3) is given by the derivative of the mean field and vanishes for $h = h_0$. Following [11] we introduce the commutator representation of B^i and B^i_0

$$B^i_{(0)} = \big[C^i, A_{(0)}(0)\big] = \big[C^i, A_{(0)}(\mu) + 2\mu h_{(0)}\big] \quad \text{(B.5)}$$

with

$$C^i = \frac{\alpha^i}{2} - \mathrm{i}r^i\partial_\tau\,. \quad \text{(B.6)}$$

First we treat the proper-time regularized sea contribution and notice that the first derivative of the exponential function is given by

$$\begin{aligned} &\frac{\partial}{\partial v^k}\,\mathrm{e}^{-sA(0;\boldsymbol{v})} \quad \text{(B.7)} \\ &\quad = -s\int_0^1 \mathrm{d}t\,\mathrm{e}^{-(1-t)sA(0;\boldsymbol{v})}\left[B^k - 2p^k p^l v^l\right]\mathrm{e}^{-tsA(0;\boldsymbol{v})}\,. \end{aligned}$$

At $\boldsymbol{v} = \mathbf{0}$ only B^k survives in the inner bracket and can be replaced by the commutator (B.5). The integral is just the commutator between C^k and $\mathrm{e}^{-sA(0)}$ (see e. g. appendix of [26])

$$\begin{aligned} \frac{\partial}{\partial v^k}\,\mathrm{e}^{-sA(0;\boldsymbol{v})}\bigg|_{\boldsymbol{v}=\mathbf{o}} &= \int_0^1 \mathrm{d}t\,\mathrm{e}^{-(1-t)sA(0)} \\ &\quad\times\,\big[C^k, -sA(0)\big]\,\mathrm{e}^{-tsA(0)} \\ &= \Big[C^k, \mathrm{e}^{-sA(0)}\Big]\,. \quad \text{(B.8)} \end{aligned}$$

The second derivative is obtained by differentiating (B.7). At $\boldsymbol{v} = \mathbf{0}$ we can apply (B.8) and get

$$\begin{aligned} &\frac{\partial^2}{\partial v^i \partial v^k}\,\mathrm{e}^{-sA(0;\boldsymbol{v})}\bigg|_{\boldsymbol{v}=\mathbf{o}} \quad \text{(B.9)} \\ &\quad = -s\int_0^1 \mathrm{d}t\,\Big[C^i, \mathrm{e}^{-(1-t)sA(0)}\Big]\,B^k\,\mathrm{e}^{-tsA(0)} \\ &\qquad + s\int_0^1 \mathrm{d}t\,\mathrm{e}^{-(1-t)sA(0)} 2p^i p^k\,\mathrm{e}^{-tsA(0)} \\ &\qquad - s\int_0^1 \mathrm{d}t\,\mathrm{e}^{-(1-t)sA(0)}\,B^k\,\Big[C^i, \mathrm{e}^{-tsA(0)}\Big]\,. \end{aligned}$$

Calculating the trace of expression (B.9) the various terms can be rearranged and simplified. The integration over t becomes trivial

$$\begin{aligned} &\mathrm{Tr}\,\frac{\partial^2}{\partial v^i \partial v^k}\mathrm{e}^{-sA(0;v)}\bigg|_{\boldsymbol{v}=\mathbf{o}} \quad \text{(B.10)} \\ &\quad = 2\mathrm{Tr}\left[s\,\mathrm{e}^{-sA(0)}\Big(p^i p^k + \frac{1}{2}\left[C^i, B^k\right]\Big)\right] \end{aligned}$$

and we get

$$\begin{aligned} \mathcal{M}^{\rm sea}_{ik} &= -\,\frac{\partial^2}{\partial v^i \partial v^k}\,\Omega^{\rm q,sea}_\Lambda(\boldsymbol{v})\bigg|_{\boldsymbol{v}=\mathbf{o}} \quad \text{(B.11)} \\ &= -N_{\rm c}\int_{1/\Lambda^2}^{\infty} \mathrm{d}s\lim_{T\to 0} T\mathrm{Tr}\left[\mathrm{e}^{-sA(0)}\left(p^i p^k + \frac{1}{2}\left[C^i, B^k\right]\right)\right. \\ &\qquad \left. -\frac{1}{2}\mathrm{e}^{-sA_0(0)}\left[C^i, B^k_0\right]\right] \end{aligned}$$

with the commutators

$$\big[C^i, B^k\big] = 2\delta^{ik}\partial_\tau^2 + \mathrm{i}\gamma^i\partial_k\left(\sigma + \mathrm{i}\gamma_5\boldsymbol{\tau}\cdot\boldsymbol{\pi}\right)\,, \quad \text{(B.12)}$$

$$\big[C^i, B^k_0\big] = 2\delta^{ik}\partial_\tau^2\,. \quad \text{(B.13)}$$

Notice that $\mathrm{Tr}\big[\mathrm{e}^{-sA_0(0)}p^i p^k\big]$ vanishes because of $p^i p^k = \frac{\mathrm{i}}{2}\big[A_0(0), r^i p^k\big]$ and the cyclic property of the trace.

Now we consider the medium contribution (16) to the inertial mass and find

$$\begin{aligned} &\frac{\partial^2}{\partial v^i \partial v^k}\,\mathrm{Tr}\,\ln A(\mu;\boldsymbol{v})\bigg|_{\boldsymbol{v}=\mathbf{o}} \quad \text{(B.14)} \\ &\quad = -2\mathrm{Tr}\left[A(\mu)^{-1}\,p^i p^k + \frac{1}{2}A(\mu)^{-1}\,B^i A(\mu)^{-1}\,B^k\right]\,. \end{aligned}$$

To evaluate the second term we apply the commutator representation (B.5) of the operator B^i and get

$$\begin{aligned} &\mathrm{Tr}\Big[A(\mu)^{-1}\,B^i A(\mu)^{-1}\,B^k\Big] \quad \text{(B.15)} \\ &\quad = \mathrm{Tr}\Big[A(\mu)^{-1}\left[C^i, A(\mu) + 2\mu h\right]A(\mu)^{-1}\,B^k\Big] \\ &\quad = \mathrm{Tr}\Big[A(\mu)^{-1}\left[C^i, A(\mu)\right]A(\mu)^{-1}\,B^k\Big] \\ &\qquad + 2\mu\,\mathrm{Tr}\Big[A(\mu)^{-1}\left[C^i, h\right]A(\mu)^{-1}\,B^k\Big]\,. \end{aligned}$$

The first term in (B.15) will be treated as in [11] yielding

$$\mathrm{Tr}\Big[A(\mu)^{-1}\,[C^i,A(\mu)]\,A(\mu)^{-1}\,B^k\Big]=\mathrm{Tr}\Big[A(\mu)^{-1}[C^i,B^k]\Big]. \tag{B.16}$$

To reformulate the second term we rewrite the commutator

$$[C^i,h]=-\frac{\mathrm{i}}{2}\{r^i,A(\mu)\}+\mathrm{i}D(\mu)^\dagger r^i D(\mu) \tag{B.17}$$

with $\{A,B\}\equiv AB+BA$ and get

$$\begin{aligned}&\mathrm{Tr}\left[A(\mu)^{-1}\,[C^i,h]A(\mu)^{-1}\,B^k\right] \\ &=-\mathrm{iTr}\Big[A(\mu)^{-1}\,B^kA(\mu)^{-1}\\ &\qquad\times\left(\frac{1}{2}\left\{r^i,A(\mu)\right\}-D(\mu)^\dagger r^i\,D(\mu)\right)\Big]\\ &=-\mathrm{iTr}\left[A(\mu)^{-1}\,\frac{1}{2}\{B^k,r^i\}\right]\\ &\qquad+\mathrm{iTr}\left[\left(D(\mu)^\dagger\right)^{-1}B^kD(\mu)^{-1}r^i\right].\end{aligned} \tag{B.18}$$

Using (B.1, B.3) we obtain

$$\frac{1}{2}\{r^i,B^k\}=\left(2r^ip^k-\mathrm{i}\delta^{ik}\right)\partial_\tau-r^i[h,p^k] \tag{B.19}$$

and

$$\begin{aligned}&\mathrm{Tr}\left[\left(D(\mu)^\dagger\right)^{-1}B^kD(\mu)^{-1}r^i\right]\\ &=\mathrm{Tr}\left[A(\mu)^{-1}\left(p^kr^iD(\mu)-D(\mu)^\dagger r^ip^k\right)\right]\\ &=\mathrm{Tr}\left[A(\mu)^{-1}\left(2r^ip^k\partial_\tau-\mathrm{i}\delta^{ik}D(\mu)+[r^ip^k,h]\right)\right].\end{aligned} \tag{B.20}$$

The last term does not contribute to the trace since h commutes with $A(\mu)^{-1}$. Altogether we have

$$\begin{aligned}\frac{\partial^2}{\partial v^i\partial v^k}\,\mathrm{Tr}\,\ln A(\mu;\boldsymbol{v})\Big|_{\boldsymbol{v}=\mathbf{o}}&=-\mathrm{Tr}\Big[A(\mu)^{-1}\\ &\times\Big(2p^ip^k+[C^i,B^k]+2\mu\left[(h-\mu)\delta^{ik}+\mathrm{i}r^i[h,p^k]\right]\Big)\Big]\end{aligned} \tag{B.21}$$

and

$$\begin{aligned}&\frac{\partial^2}{\partial v^i\partial v^k}\,\mathrm{Tr}\,\ln A_0(\mu;\boldsymbol{v})\Big|_{\boldsymbol{v}=\mathbf{o}}\\ &=-\mathrm{Tr}\left[A_0(\mu)^{-1}\left([C^i,B_0^k]+2\mu(h_0-\mu)\delta^{ik}\right)\right]\end{aligned} \tag{B.22}$$

with the commutators $[C^i,B^k]$ and $[C^i,B_0^k]$ given in (B.12, B.13). Finally we get

$$\begin{aligned}\mathcal{M}_{ik}^{\mathrm{med}}&=-\frac{\partial^2}{\partial v^i\partial v^k}\Omega^{\mathrm{q,med}}(T,\mu;\boldsymbol{v})\Big|_{\boldsymbol{v}=\mathbf{o}}\\ &=-N_{\mathrm{c}}T\mathrm{Tr}\Big[A(\mu)^{-1}\left(p^ip^k+\frac{1}{2}[C^i,B^k]\right)\\ &\qquad-\frac{1}{2}A_0(\mu)^{-1}[C^i,B_0^k]\Big]\\ &\quad+N_{\mathrm{c}}\lim_{T\to0}T\mathrm{Tr}\Big[A(0)^{-1}\left(p^ip^k+\frac{1}{2}[C^i,B^k]\right)\\ &\qquad-\frac{1}{2}A_0(0)^{-1}[C^i,B_0^k]\Big]\\ &\quad-N_{\mathrm{c}}T\mathrm{Tr}\Big[A(\mu)^{-1}\,\mu\left((h-\mu)\delta^{ik}+\mathrm{i}r^i[h,p^k]\right)\\ &\qquad-A_0(\mu)^{-1}\mu(h_0-\mu)\delta^{ik}\Big].\end{aligned} \tag{B.23}$$

References

1. Nambu, Y., Jona-Lasinio, G.: Phys. Rev. **122**, 345 (1961); **124**, 246 (1961)
2. Christov, C.V., Blotz, A., Kim, H.C., Pobylitsa, P.V., Watabe, T., Meißner, T., Arriola, E.R., Goeke, K.: Prog. Part. Nucl. Phys. **37**, 1 (1996)
3. Alkofer, R.,Reinhardt, H., Weigel, H.: Phys. Rep. **265**, 139 (1996)
4. Vogl, U. and Weise, W.: Prog. Part. Nucl. Phys. **27**, 195 (1991)
5. Hatsuda, T., Kunihiro, T.: Phys. Rep. **247**, 221 (1994)
6. Jaminon, M., Ripka, G., Stassart, P.: Nucl. Phys. A**504**, 733 (1989)
7. Berger, J., Christov, C.V.: Nucl. Phys. A**609**, 537 (1996)
8. Birse, M.C.: J. Phys. G **20**, 1537 (1994)
9. Christov, C.V., Goeke, K.: Nucl. Phys. A**564**, 551 (1993)
10. Ring, P., Schuck, P.: The Nuclear Many-Body Problem. Berlin, Heidelberg, New York: Springer 1980
11. Pobylitsa, P.V., Arriola, E.R., Meißner, T., Grümmer, F., Goeke, K., Broniowski, W.: J. Phys. G**18**, 1455 (1992)
12. Stratonovich, R.L.: Dokl. Akad. Nauk S.S.S.R **115**, 1907 (1957)
13. Hubbard, J.: Phys. Rev. Lett. **3**, 77 (1959); Proc. Roy. Soc. A**276**, 238 (1963); Proc. Roy. Soc. A**277**, 237 (1964); Proc. Roy. Soc. A**281**, 401 (1964)
14. Sieber, P., Meissner, Th., Grümmer, F., Goeke, K.: Nucl. Phys. A**547**, 459 (1992)
15. Watabe, T, Toki, H.: Prog. Theor. Phys. **87**, 651 (1992)
16. Schwinger, J.: Phys. Rev. **82**, 664 (1951)
17. Eguchi, T.: Phys. Rev. **D14**, 2755 (1976)
18. Meissner, T., Goeke, K.: Nucl. Phys. A**524**, 719 (1991)
19. Wünsch, R., Goeke, K., Meissner, Th.: Z. Phys. A**348**, 111 (1994)
20. Kahana, S., Ripka, G.: Nucl. Phys. A**429**, 462 (1984)
21. Schlienz, H., Weigel, H., Reinhardt, H., Alkofer, R.: Phys. Lett. B**315**, 6 (1993)
22. Brown, G.E., Rho, M.: Phys. Rev. Lett. **66**, 2720 (1991)
23. Reinhardt, H.: Nucl. Phys. A**503**, 825 (1989)
24. Bedaque, P.F.: Phys. Lett. B**387**, 1 (1996)
25. Christov, C.V., Arriola, E.R., Goeke, K.: Nucl. Phys. A**556**, 641 (1993)
26. Veltman, M.: Diagrammatica: The Path to Feynman Diagrams, Cambridge Lecture Notes in Physics 4. Cambridge: Cambridge University Press 1994